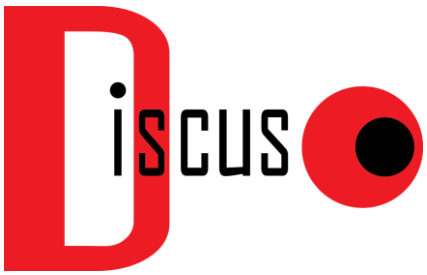

D7.1

Power Consumption Studies

Dissemination Level: PU

- **Dissemination level:**

  PU = Public,
  RE = Restricted to a group specified by the consortium (including the Commission Services),
  PP = Restricted to other programme participants (including the Commission Services),
  CO = Confidential, only for members of the consortium (including the Commission Services)

Abstract:

This “power consumption studies” deliverable is a WP7 deliverable and therefore considers only the core network.

1. We describe initial version of routing and spectral allocation, featuring an initial version of flex-grid developed for this deliverable. A basic model of fixed-grid was also created. We describe strategies to optimize power including non-uniform traffic allocation, hibernating operation, and static and dynamic spectrum allocation.
2. We describe power consumption models created for the photonic and packet transport equipment of the DISCUS core network. For the photonic equipment, the optical functionalities required in the core nodes and configurable transponders are identified. The functionalities are grouped into network system boards, and typical power consumption of such boards are evaluated. Similarly, for the packet transport equipment, i.e. the MPLS-TP packet switch, a set of line, client and switching boards that fulfil DISCUS service requirements are identified.
3. We describe energy efficient resilient strategies for core networks that leverage on the inherent tradeoff between level of achievable power savings and other important network performance parameters such as cost, blocking probability, and the actual level of protection. We also consider the impact of energy efficient strategies, such as frequent component state transition, on lifetime of core components.

(M15, KTH, TI, ASTON, editor ASTON, dissemination level: Public).

Authors:

Name	Affiliation
Marco Schiano	Telecom Italia
Marco Quagliotti	Telecom Italia
Paolo Monti	KTH
Farsheed Farjady	ASTON

Internal reviewers:

Name	Affiliation
David Payne	TCD/ASTON
Elias Giacoumidis	ASTON

Due date: 31.01.2014

COPYRIGHT

The DISCUS Consortium consists of:

Participant Number	Participant organization name	Participant org. short name	Country
Coordinator			
1	Trinity College Dublin	TCD	Ireland
Other Beneficiaries			
2	Alcatel-Lucent Deutschland AG	ALUD	Germany
3	Coriant R&D GmbH	COR	Germany
4	Telefonica Investigacion Y Desarrollo SA	TID	Spain
5	Telecom Italia S.p.A	TI	Italy
6	Aston University	ASTON	United Kingdom
7	Interuniversitair Micro-Electronica Centrum VZW	IMEC	Belgium
8	III V Lab GIE	III-V	France
9	University College Cork, National University of Ireland, Cork	Tyndall & UCC	Ireland
10	Polatis Ltd	POLATIS	United Kingdom
11	atesio GMBH	ATESIO	Germany
12	Kungliga Tekniska Hoegskolan	KTH	Sweden

TABLE OF CONTENTS

TABLE OF FIGURES

1 Introduction

POWER consumption is becoming an important consideration in telecommunications networks because of ever increasing quantity of network equipment, and increasing line rates, and is an important contributor to operational expenditure (OPEX). Currently the world's ICT uses 1500 TWh of electricity annually [1], equal to all the electric generation of Japan and Germany combined, and as much electricity as was used for global illumination in 1985. A recent study [2] has stated that the combined electricity demand of the internet/cloud (data centres and telecommunications network) globally in 2007 was approximately 623 TWh. If the cloud were a country, it would have the fifth largest electricity demand in the world (after US, China, Russia, and Japan). In broadband enabled countries that have an average access rate of the order of 30 Mb/s [3]-[4], energy consumption of the Internet is approximately 1% of the total electricity consumption. Power consumption related to ICT is approximately 2%-10% of worldwide power consumption. ICT equipment accounts for about 10% of the UK's total electricity consumption [5]. In 2000, it was found that the total national energy consumption of the Internet in the US was about 1%-2% of total electricity consumption [3][6]. The increasing energy costs have serious environmental impact on the Green House Gases (GHG) emissions. Gartner, the ICT research and advisory company, in 2007 estimated that the manufacture of ICT equipment, its use and disposal accounts for 2% of global CO2 emissions which is equivalent to the aviation industry [7] and the 2% figure was later confirmed in [8]. In 2007, the total footprint of the ICT sector, including personal computers (PCs) and peripherals, telecoms networks and devices and data centres, was 830 MtCO2e, about 2% of the estimated total emissions from human activity that year. Unless we change the architecture of communications networks to have much greater energy efficiency eventually it will be the energy consumption rather than cost of component equipment that limits the continued growth of the Internet.

This deliverable deals with the power consumption of the core network only. Section 2 describes a power consumption study using a flex-grid routing and spectrum allocation model that was especially developed for this deliverable. Section 3 describes a more in-depth power consumption model of photonic and packet transport equipment. These models can be used to evaluate the core network power consumption as a function of the traffic through the core network. Section 4 describes energy efficient resilient strategies for core networks that leverage the inherent trade-off between the level of achievable power savings and other important network performance parameters such as cost, blocking probability, and the actual level of protection provided. In addition, the impact of energy efficient strategies, i.e. frequent component state transitions used to save power (e.g. turning equipment off when not carrying traffic) on the lifetime of core components is examined.

2 Power Consumption Modelling of Flex-grid and Fixed-grid Core Networks

2.1 Introduction

In this section we consider power consumption optimisation in flex-grid networks. The strategies investigated for power consumption optimization include hibernating operation, non-uniform traffic allocation, and dynamic traffic, and dynamic spectral allocation. A routing and spectral allocation algorithm on a 6.25 GHz granularity spectrum grid was developed for this deliverable. We describe the progress of a flex-grid core model, and a fixed-grid model with 37.5 GHz grid spacing. These models will be further developed and results shall be reported in other deliverables.

2.2 Advantages of Flexgrid

As the Internet traffic grows, more efficient utilization of optical fibre spectrum is required for extremely high data rate transmission. Because of flat-rate pricing models for customers, and the fact that traffic demands are steadily increasing in volume and bandwidth, the network service providers face strong pressure to improve their networks whilst also having to reduce the cost per bit. The cost reduction in WDM systems is achieved by sharing optical components among WDM channels, for example by using in-line optical amplifiers and using common optical fibres for transport and dispersion management. The reduction of cost per bit is also achieved by increasing system reach, increasing the aggregate WDM capacity, and increasing per-channel data rates. Increasing reach also enables express channels so that through traffic traversing core nodes does not need terminating and OEO conversion. This can be an even more important mechanism for cost reduction particularly if it also reduces electronic packet processing.

In traditional DWDM systems, the optical spectrum in the C-band consists of about 4.4 THz divided into rigid 50 GHz spectrum slots. This forms the “ITU wavelength grid”, where the centre frequencies of neighbouring channels have a rigid spectrum spacing of 50 GHz. The channel spacing of DWDM can support various grid sizes, such as 12.5 GHz, 25 GHz, 50 GHz, or 100 GHz. 50 GHz channel spacing is typically chosen for DWDM. ITU-T has recently revised the G.694.1 recommendation and included the definition of a flexible DWDM grid.

Service providers are beginning to implement high bit rate channels such as 40 Gb/s and 100 Gb/s and even 400Gb/s. To transmit 100 Gb/s within the 50 GHz fixed grid DWDM it would be possible to use advanced modulation formats and photonic techniques. However for greater traffic speeds, such as 400 Gbit/s and 1 Tbit/s [9], the necessary spectral widths using standard modulation formats become too broad to fit into the 50 GHz grid. One strategy to overcome this problem could be to increase the width of the fixed-grid from 50 GHz to 100 GHz. However, the disadvantage with using a wider grid would be fewer wavelength channels, and backward compatibility with lower bit-rate channels which would use up 100GHz channel each, thus wasting spectral bandwidth, and reducing utilization efficiency of spectrum resources. Another strategy would be to use

higher spectral efficiency modulation formats such as QPSK. However this results in shorter optical reach because of increased OSNR requirements. Another solution is to use inverse multiplexing, where higher rate channels are sent over a number of wavelengths in parallel in the 50 GHz channels. This allows the lower rate channels to be transmitted more efficiently but at the expensive of greater complexity for the higher rate channels. The effect of inverse multiplexing on the blocking probability compared to flex-grid shall be studied further in later deliverables.

An alternative solution receiving much attention today is to use a flex-grid approach. Spectrum allocation in flex-grid systems differs from DWDM channel assignment in that the channel width is not rigidly defined but can be tailored to the required baud rate of the transmitted channel. Using flex-grid [9]-[11] optical networks can assign variable channel bandwidths in multiples of a much smaller granularity (e.g. 12.5 GHz). Elastic Optical Paths (EOPs) have dynamic bandwidth variation functionality to dynamically expand or contract channel bandwidths in integer numbers of 12.5 GHz slots. In fixed-grid for low channel line rates, gaps between neighbouring wavebands become large, especially if the grid spacing is large, and spectrum utilisation can be inefficient.

2.3 Power Aware Routing & Spectral Allocation

We consider the optical network shown in Figure 2-1, consisting of wavelength routers interconnected with fiber links. Note that in the DISCUS flat optical island architecture the core network would consist of a much larger number of nodes (possibly ~100). This small network is used to demonstrate and test the model. The distances in km are displayed on the links.

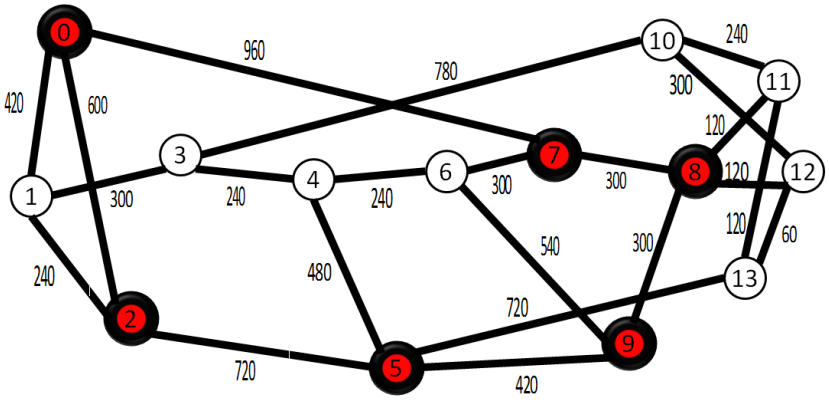

Figure 2-1: Showing the core network: solid circles are the subset of core nodes {0, 2, 5, 9, 8, and 7} that have 1x (uniform allocation) or 10x (non-uniform allocation) probability of being selected as source or destination nodes.

Figure 2-2 shows a flow diagram of the algorithm. The network can be represented by a graph $G=(N,L,\Omega)$, where $N=\{n_0,n_1,\ldots,n_{N-1}\}$ is a set of nodes, $L=\{l_0,l_1,\ldots,l_{m-1}\}$ is a set of links, and $\Omega=\{\omega_0,\omega_1,\ldots,\omega_{\Phi-1}\}$ is a set of wavelengths or spectrum slices/slots available in each link.

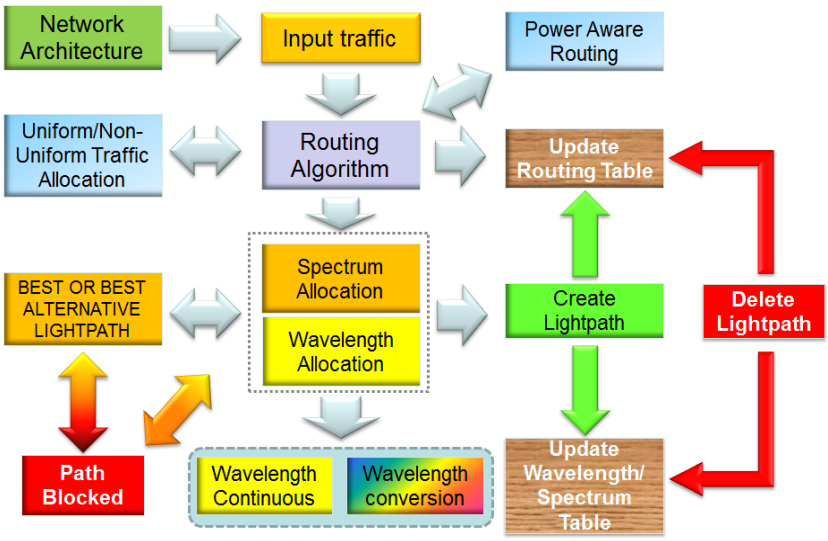

Figure 2-2: Flow diagram of routing and wavelength allocation program.

2.3.1 Routing Algorithm

A set of Δ traffic demands $T=\{T_0,T_1,T_2\cdots T_\Delta\}$ is offered to the network; each connection request is represented by $T_r=(s_r,d_r,\alpha_r,\delta_r,\beta_r)$, where s_r and d_r are the source and destination nodes for a request r respectively, α_r and δ_r are the set-up and tear-down times of the demands respectively, and $t_r=\delta_r-\alpha_r$ is the holding time, and β_r is the bandwidth requested.

The source and destination nodes are chosen with uniform distribution, that is all nodes are equally likely and also the bandwidth allocation for the requests between these nodes is chosen with uniform distribution, 0-200 Gbps is used in the results in this section. Alternatively the program can select quantised bandwitdhs with uniform distribution, at present, bandwidths of e.g. 10Gbps, 40Gbps, 100 Gbps, 200Gbps are used. The actual shape of the distribution in both cases needs to be further examined. The holding times and inter-arrival times are allocated according to Poisson exponential distribution. The traffic allocation can be considered to be uniform and non-uniform, where "uniform" traffic allocation means that the probability of the nodes being selected as source or destination nodes is uniform, and "non-uniform" traffic means that the probability of certain nodes being selected for source and destination is increased (e.g. 10x in this case). This allows for some variation of traffic matrix dependencies to be studied. More realistic models for traffic matrices such as "Gravity" models will be studied later and the results will be presented in later deliverables.

The algorithm first tries to create routing tables that specify a first choice path and a number of alternative paths. It uses a shortest path first (SPF) algorithm that generates routing tables that include a least-cost path and a specified number of alternative paths. The algorithm selects the least-cost path if available. If the least-cost path is unavailable, it selects the next least-cost path. To calculate the least cost parameter it considers the distance, power consumption, and number of hops of the lightpaths. The number of hops refers to the number of links traversed in the

optical network, and is used as a tie-breaker only when more than one paths have the same cost.

A simple power consumption model is assumed for the lightpaths including the power consumption of the end routers and the amplifiers along the path. The power consumption of source and destination nodes due to electronic routers is assumed to be 5W/Gbps [17]. The power consumption of the intermediate nodes is assumed to be negligible. We have not included the power consumption of the metro-core equipment. For the transmission links we assume that each fiber has EDFAs consuming 8W and are spaced with 80 km span lengths.

2.3.2 Wavelength Allocation

Following the routing allocation, either wavelength allocation or spectral allocation can be applied. The wavelength allocation algorithm checks the availability of the first available wavelength in all the links along the path. For transparent connections, the allocation is according to a wavelength continuity constraint, with the same wavelength being used in all the links along the lightpath. Note that each individual fibre carries an equal number of wavelengths. The wavelength allocation algorithm in the program can also allow wavelength conversion, allowing sparse or full wavelength conversion in the network to be examined.

The program can allow any number of fibres to be allocated per unidirectional link, although for the results shown in this section it is assumed there is only one fibre allocated per unidirectional link. For the multiple fibre case (results not shown), when assigning a wavelength, the algorithm attempts to use the first wavelength in the original fibre. If this wavelength is in use, it then chooses the same wavelength in an overlay fibre. If the wavelength is unavailable in all the overlay fibres the algorithm attempts to use the next available wavelength in the original fibre.

2.3.3 Spectral Allocation

In addition to the wavelength allocation algorithm, we have now developed a spectral allocation algorithm. In this case, the spectrum is divided into 6.25 GHz slice granularities [13]-[16]. Once the bandwidth of a traffic request is known, modulation formats are applied to optimize the spectrum for the particular reach. The resulting baud-rate is then allocated spectrum in the necessary links along the lightpath, with the minimum spectrum being allocated having a slot size of 12.5 GHz (two slices i.e. ±6.25 GHz resolution). For transparent connection the spectral allocation is the same in all the links along the lightpath, according to spectral continuity.

2.4 Results

For large traffic volumes with high numbers of >100Gb/s channels, there may be significant spectral efficiency advantage in using flex-grid. The efficiency benefits of flex-grid would be even greater in a network environment than in a point-to-point link, because fixed-grid uses multiple inversed multiplexed channels and consequently may result in more optical path blockage. The relative blocking will

be quantified in later studies. Inverse multiplexing is less spectrally efficient than contiguous EOPs. The benefits of flex-grid become even greater when higher order transmission techniques are employed and channel baud-rates are reduced. Flex-grid can potentially reduce network blocking by consolidating available network resources enabling better network maintenance e.g. using spectral defragmentation. However spectral defragmentation requires spectrum channel re-assignment which can cause interruptions when applied to traffic carrying light paths therefore the full pragmatic spectral efficiency benefits of flex-grid require further evaluation. Flex-grid has higher granularity than fixed-grid, and potentially allowing closer fit to the allocated spectrum, and adaptive allocation of spectrum according to traffic variations.

2.4.1 Flexgrid Spectral Allocation

Figure 2-3 shows results of spectral allocation of this network, where the spectrum allocation for each link is shown. The 44 links in the network refer to two links per physical path, one link for each direction. The traffic requests each have bandwidths between 0-200 Gbps with modulation formats subsequently applied. This flex-grid allocation can allocate spectrum resources elastically, according to traffic demands. The spectral slices of the spectrum grid have 6.25 GHz granularity. It is observed that the same spectrum is allocated in multiple links that are used by the lightpaths to transparently traverse from source to destination.

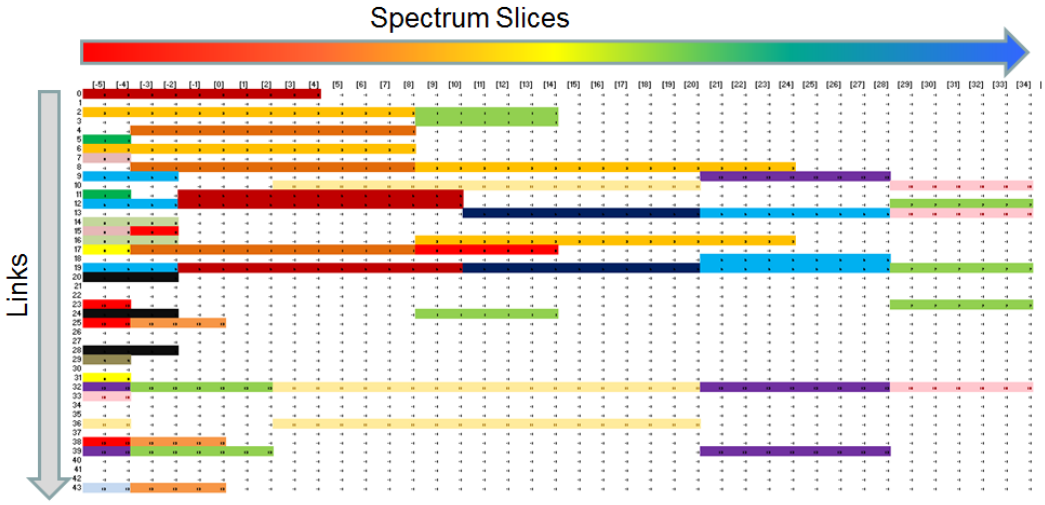

Figure 2-3: Flexgrid spectral allocation in the 44 unidirectional links in the network, for 0-200 Gb/s traffic allocated and optimised for the reaches with various modulation formats. The various colours are used to distinguish between the various channels. Guardbands between channels are to be included in later versions of the model. The spectral slice grid is 6.25 GHz granularity.

Various channel size allocation are observed in Figure 2-3. The large channels can be considered to be super-channels allowing handling of large demands that could not be served by a single optical channel. The super-channels consist of multiple closely spaced channels that traverse the network in one unit, and can be demultiplexed at the receiver. By using similar higher order modulation schemes the smaller channels are carried more efficiently than fixed-grid because they don't

use up the entire 37.5 GHz or 50 GHz grid. At present guardbands between channels haven't been included in the model. These will be developed in later versions of the model.

Figure 2-4 shows that the algorithm can modify a bandwidth allocation and redistribute channels if required.

Figure 2-4: Reallocation of bandwidth for a particular channel.

2.4.2 Fixedgrid Spectral Allocation

Regarding fixed-grid only an initial model has been constructed for this deliverable. Figure 2-5 shows the fixed-grid allocation. The channels here are on a regularly spaced grid, assuming a 37.5 GHz grid. The lightpaths shown in Figure 2-5 are 25 Gbps channels with no modulation formats. We note that the available spectrum is used more quickly than flex-grid, because for smaller channels the complete 37.5GHz is used, and for larger channels it is necessary to use inverse multiplexing and multiple lightpaths. Later versions of the model will include larger channels as well as modulation formats, and guardbands. Once these are included a fair comparison between the flex-grid and fixed-grid can be made. These results shall be presented in later deliverables.

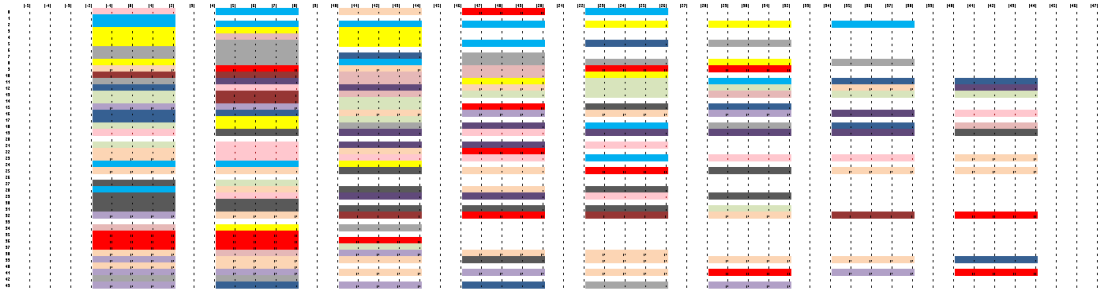

Figure 2-5: Very basic version of fixedgrid showing 25 Gbps channels in a 37.5GHz grid. Guardbands between channels are to be included in later versions of the model.

The rest of the results shown in this chapter all assume flex-grid implementation.

2.4.3 Effect of Dynamic Traffic Allocation

We now consider what happens when the traffic allocation in the flex-grid network is dynamic, i.e. when lightpaths have limited lifetimes. **Error! Reference source not found.** shows that dynamic traffic allocation reduces the power consumption as expected. The dynamicity of the traffic is defined as average

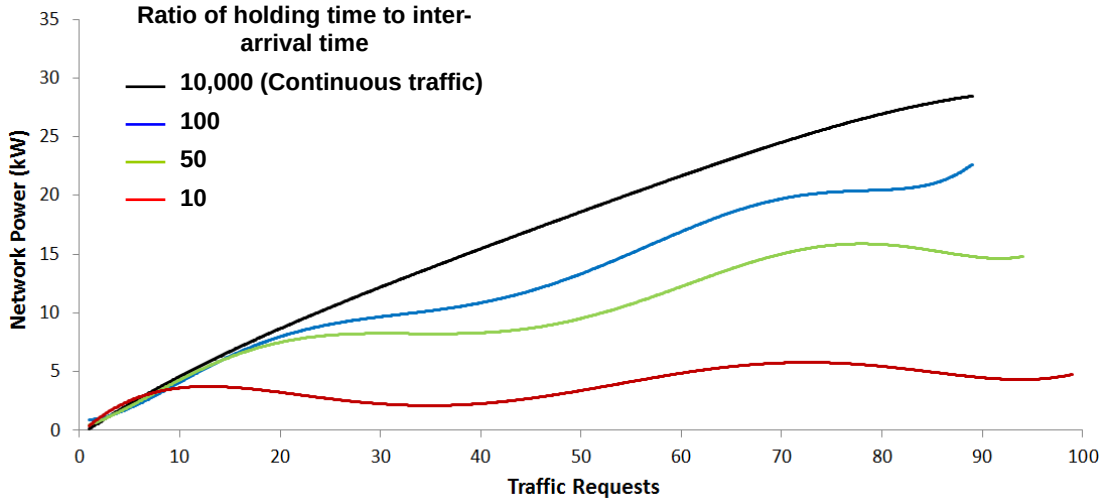

Figure 2-6 Comparison between dynamic and static operation with hibernating-mode amplifier operation using Uniform traffic.

holding time/average inter-arrival time).

The power consumption of the nodes is shown in Figure 2-7 below, showing that dynamic allocation reduces the power consumption considerably.

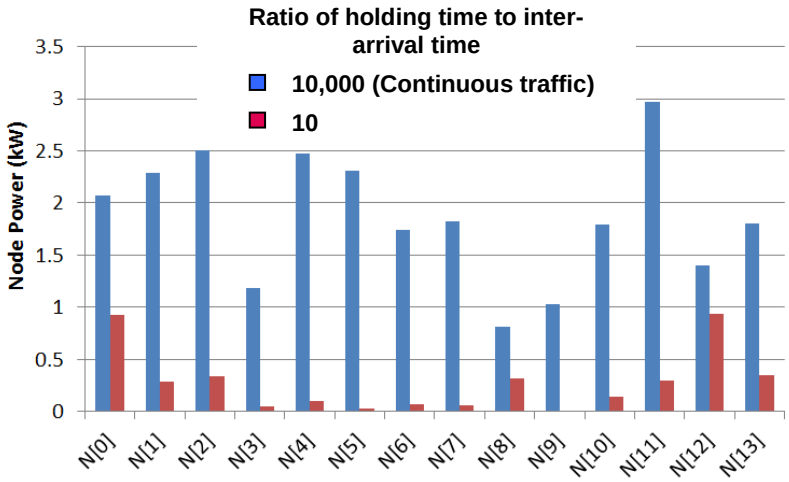

Figure 2-7: Node power consumption reduction for dynamic (10 Erlangs) operation compared with static operation (10000 Erlangs) assuming uniform traffic.

2.4.4 Effect of Modulation Formats on Power

In the results shown in this chapter, we have used the modulation formats of Table 1 (obtained in Deliverable D7.2) to make efficient use of the spectrum. We have assumed traffic requests ranging from 0 to 200 Gbps.

Table 1: Modulation Formats [18]

Symbol	Maximum Reach	Spectral Efficiency
DP-BPSK	2430	1.33
DP-QPSK	1170	2.67
DP-16QAM	270	5.33

Figure 2-8 shows a comparison of the effect on power consumption using advanced modulation formats, and not using advanced modulation formats. It is shown that advanced modulation formats reduce the power consumption due to the narrower spectrums.

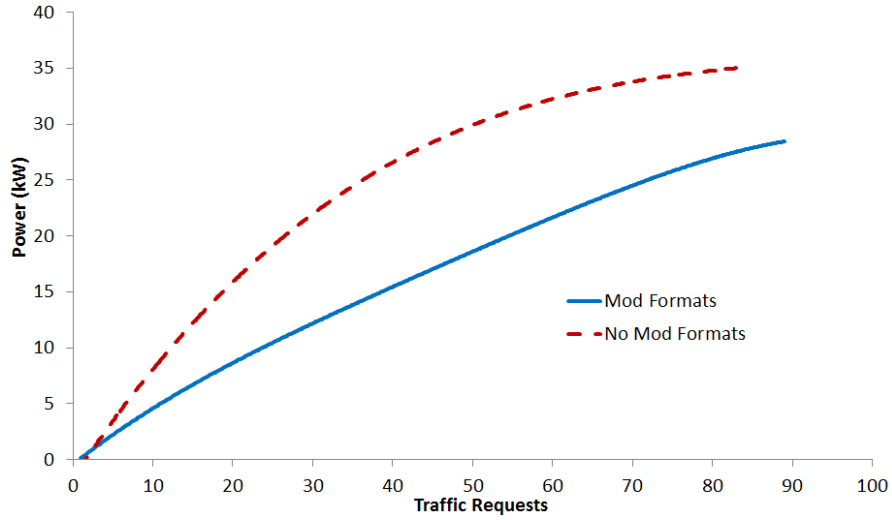

Figure 2-8: shows the effect of including modulation formats on the power consumption compared with not using modulation formats.

2.4.5 Effect of Dynamically Switched Amplifiers

We have assumed that the EDFAs can either be switched on all the time ('awake' mode) or switched off ('hibernating' mode) at the start of the traffic allocation or when not in use. For example, at the start of the connection allocation in the network this results in low power consumption. In the hibernating mode operation, amplifiers are switched on when the first wavelength is used in a fiber. Each lightpath is assumed to have a limited lifetime. Figure 2-9 shows a comparison between the two modes of operation.

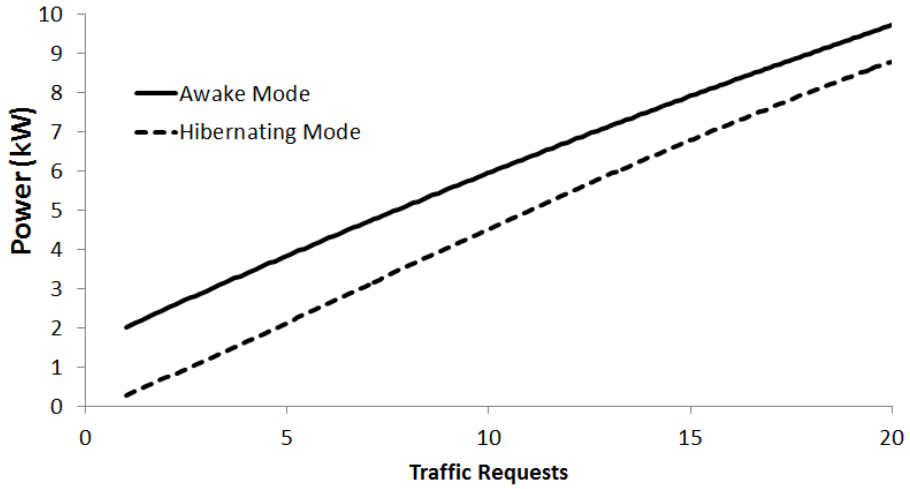

Figure 2-9: Comparison between hibernating and awake amplifier operation using Uniform 10000 Erlang traffic.

2.4.6 Non-Uniform Traffic

Figure 2-10 shows the effect of non-uniform traffic on the power consumption of the individual nodes. As the network expands, there may be increasing practical problems with supplying large amounts of energy to large network nodes. Non-

uniform traffic allocation was considered either to localize or distribute power consumption in the network. Note that we are not claiming here that there is any net saving in power consumption, only a re-distribution of power between the nodes. This results in only a few nodes having high power consumption and the majority of nodes having low power consumption. Figure 2-10 shows the case of localizing power in certain nodes in which non-uniform traffic results in 78% reduction in power consumption requirement for majority of the core nodes. This type of approach may be useful to prevent power shortages in network implementations where each node location is constrained by a limited electricity power supply, for example areas with large populations. The localization of traffic deeper in the network allows cost-effective provisioning of additional resources to increase network capacity efficiently. This type of approach can be considered in certain situations where power consumption of network nodes needs to be distributed and equalized between the nodes to result in low power consumption in all nodes. Therefore this type of strategy can allow power consumption of various nodes to be tailored depending on the availability of electricity power supply, although the exact application of this strategy is yet to be determined.

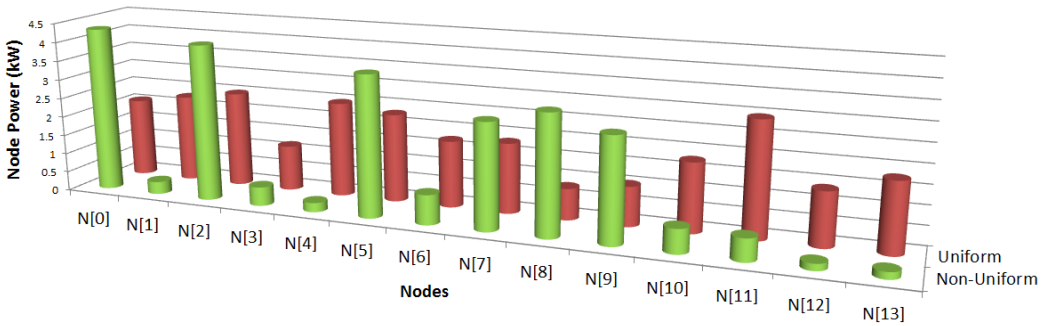

Figure 2-10: Non-Uniform traffic at the indicated nodes leads to increase in their power consumption and reduction in power consumption in the other nodes. Comparison of power distribution with uniform traffic model.

2.5 Summary/Conclusions

In this section, we examined the power consumption optimization in flex-grid networks. Some of the strategies investigated for power consumption optimization include hibernating operation, non-uniform traffic allocation, and dynamic traffic and spectral allocation. We have developed an initial version of flex-grid, and a basic version of a fixed-grid model. These will be further developed as the project progresses and shall be reported in later deliverables. Later versions of the flexgrid and fixedgrid models will include guardbands between channels, and the fixed-grid model will include modulation formats and inverse multiplexing. A simple power consumption model was assumed for this routing and spectral allocation.

In the next section we define a more comprehensive flex-grid power consumption model for the two network layers in the DISCUS network based on flex-grid ROADM and MPLS-TP switches starting from network functionalities and components at system board level. Based on these models, it is possible to calculate the network power consumption.

3 Power Consumption of Photonic and Packet Transport layer

3.1 Introduction

The DISCUS core network architecture is composed of a photonic layer and a Packet Transport layer. These two network layers are based on flexgrid ROADM and MPLS-TP switches respectively as described in deliverables D2.1 and D6.1.

The purpose of this section is to define a power consumption model for these network layers starting from network functionalities and components at system board level.

As a first step, a detailed functional block diagram is elaborated for flexgrid ROADM, configurable transponders and MPLS-TP switches considering all equipment functions required to support the network services envisaged in deliverable D6.1. Second, components or functions are grouped into boards according to the system technology state of the art today and the predictable future improvements. Finally, the power model of each board is developed based on power consumption data available in the literature or extrapolated from systems data sheets.

Based on these models, one can calculate the network power consumption once the nodes and links configuration is known.

3.2 Core Network Photonic Layer

In this sub-section, a Flexgrid ROADM and configurable transponders functional model is presented together with the related power consumption model.

3.2.1 Flexgrid ROADM

Flexgrid ROADM functions can be subdivided into WSS Line Interfaces and Add/Drop (A/D) functions.

Line interfaces functional scheme is shown in Figure 3-1.

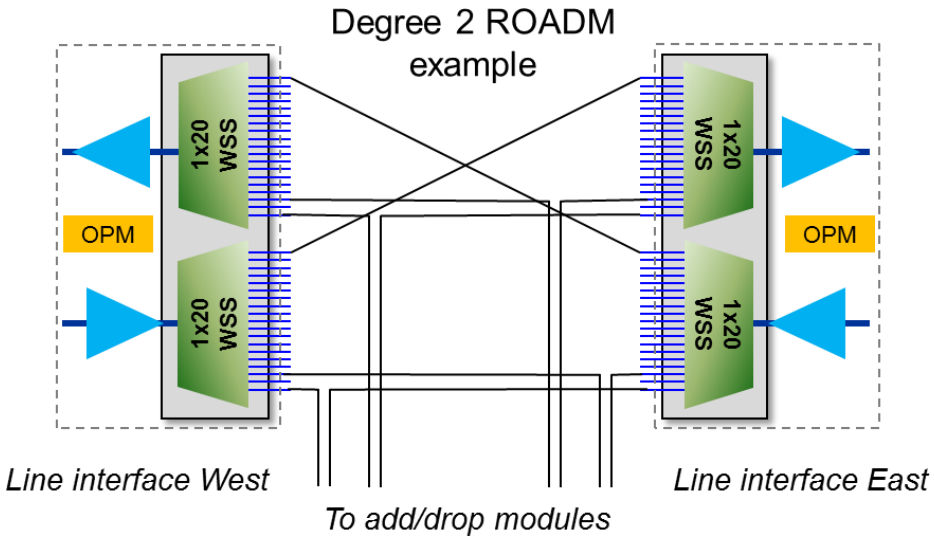

Figure 3-1: functional scheme of ROADM line interfaces. A degree 2 ROADM example is shown.

In this example each line interface encompasses two 1x20 flexgrid WSS connected in a route-and-select architecture. This architecture is mandatory when high port count WSS components are used because of the prohibitive insertion loss of the alternative architecture, the so called broadcast-and-select, where a passive power splitter and a WSS are used instead of a couple of WSS. Line interfaces also include two Erbium Doped Fibre Amplifiers (EDFAs) used as booster amplifier and pre-amplifier for the line optical signal. Finally, Optical Performance Monitoring (OPM) functions are included to provide real-time measurement of the line signal optical spectrum.

Add/Drop functions used in DISCUS are of three kinds:

- Colourless only;
- Colourless and Directionless;
- Colourless Directionless and Contentionless.

Colourless A/D functional scheme is shown in Figure 3-2.

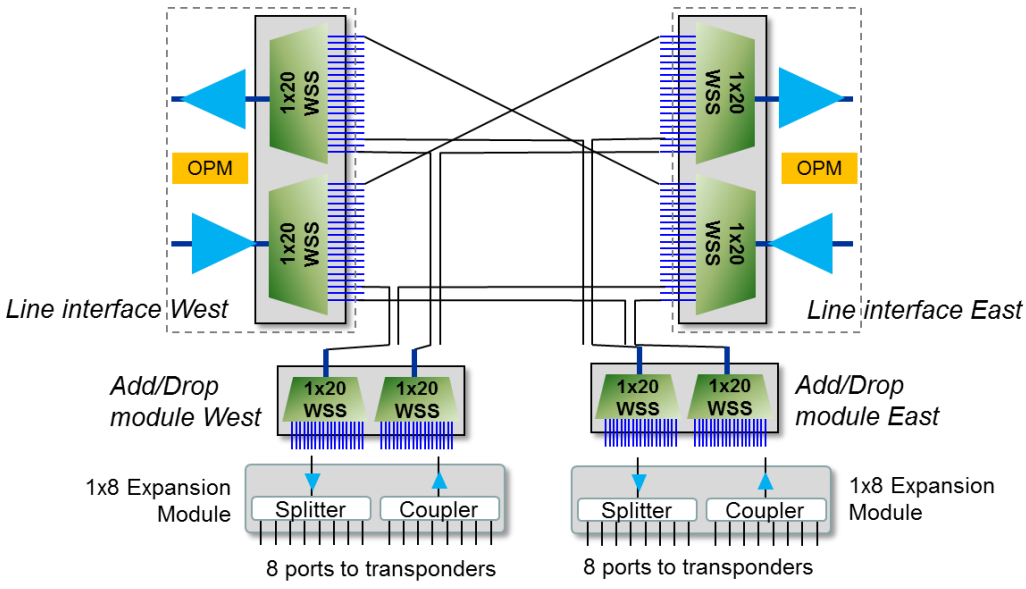

Figure 3-2: Colourless only A/D functional scheme.

In Colourless only Add/Drop (A/D) functions, 1x20 WSS are used as A/D components and are connected to a fixed line interface. WSS are used instead of fixed MUX/DEMUX filters to provide tunability of A/D wavelength, i.e. the Colourless functionality. Additional Amplified Splitter and Couplers (ASC) functions are envisaged to increase the number of A/D ports otherwise limited to 20 by the WSS itself. This A/D architecture forwards traffic to a fixed direction only.

Colourless and Directionless A/D functional scheme is shown in Figure 3-3.

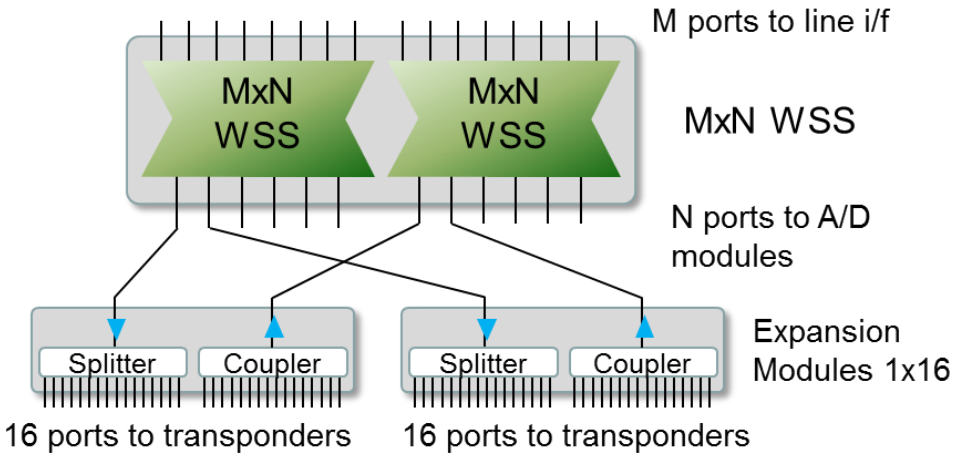

Figure 3-3: Colourless and Directionless A/D functional scheme.

In Colourless and Directionless A/D functions, MxN WSS are used instead of a couple of conventional 1xN WSS interconnected by the common port, which is the typical architecture used today. The advantage of using MxN WSS instead of two 1xN is the reduced insertion loss that avoids any additional amplification stage. MxN WSS are not yet commercially available but they are in the product roadmaps of major component manufacturers. The MxN WSS is connected to all line interfaces to ensure the Directionless functionality, and to 1x16 amplified splitter coupler (ASC) modules that provide as many A/D ports as needed in the node. This A/D architecture cannot handle two or more wavelength of the same colour because of the internal structure of the MxN WSS (they are effectively 1xM and 1xN WSS back to back), i.e. it's not Contentionless.

Colourless Directionless and Contentionless A/D functional scheme is shown in Figure 3-4.

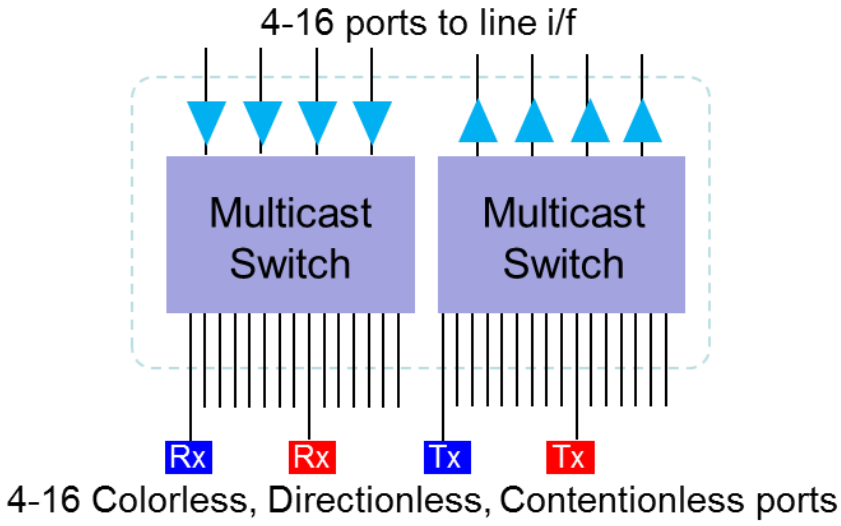

Figure 3-4: Colourless Directionless and Contentionless A/D functional scheme.

In Colourless Directionless and Contentionless A/D functions, Amplified Multicast Switches (MSC) are used instead of WSS. The internal architecture of a Multicast Switch provides a complete separation of A/D optical paths for each A/D port and therefore it can handle as many lambdas of the same colour as the number of A/D ports. This is the most flexible A/D scheme, and will become commercially available in the next few years. For the multicast function to be non wavelength selective it has to be a power splitter and therefore will have a 10log(N) loss where N is the number of I/O ports hence the need for the pre or post amplifiers to compensate for this loss.

The line and Add/Drop functions described before can be grouped into boards that are the elementary components of network systems. There are 7 kinds of boards envisaged for the DISCUS flex grid core network as shown in

Figure 3-5.

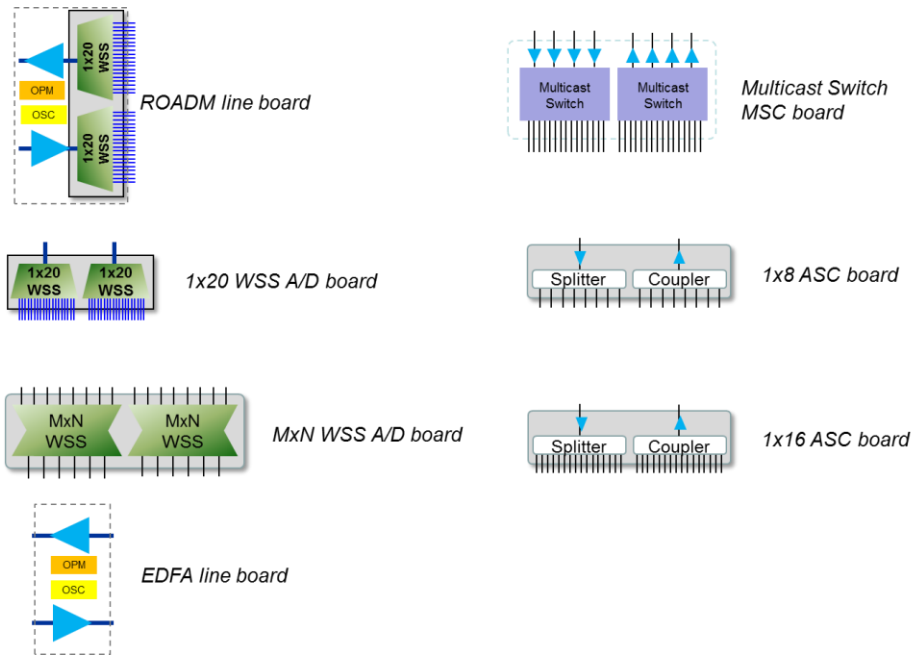

Figure 3-5: line and A/D optical functions grouped into system boards.

This subdivision of optical functions into boards is based on the most advanced component technology of today that allows housing complex optical subsystems onto a single board. The EDFA line board that has not been described before is simply the board with line amplification functions that are required in network amplification sites. The optical supervisory channel (OSC) functions that are included in line boards are the OSC functions that are required in any optically amplified link to monitor line optical amplifiers and to transport out-of-band control and management information even in case of fault of optical amplifiers.

The power consumptions of such boards can be modelled as follows.

The model is based on shelves that host the system boards defined above. Two shelf sizes with 32 and 16 slots respectively can be assumed, each with its typical power consumption that include the power needs of shelf control, communication and fan units. This basic consumption is independent from the number of installed boards on the shelf.

Each board shown in

Figure 3-5 is characterized by its power requirement and required slots (one or more). In case of ROADMs that require more than 32 slots multi-shelf configuration can be used.

The shelves are also used to host the configurable transponders (see the section 3.2.2).

The power model of the boards is based on a breakdown of each board in some elementary optical and electronic functions, each characterised by its own consumptions. These basic functional elements with their identifiers are reported in Table 3-1.

Table 3-1: Power consumption of basic sub-board functional elements

Sub-board functional elements	Identifier	Power Consumption (W)
Basic control of board	P_BCB	30
WSS module (any type)	P_WSS	20
Multicast Switch (MSC, any type)	P_MSC	5
EDFA small gain amplifier for ASC and MSC (single fibre)	P_OAN	5
EDFA single stage fixed gain (preamplifier)	P_OAP	25
EDFA dual stage variable gain (booster)	P_OAB	35
Optical Performance Motoring	P_OPM	5
Optical Supervisory Channel	P_OSC	5

In Table 3-2 the formulas used to compute the power consumption of system boards are reported. The active elements that allow the spectral filtering and switching are supposed to consume a certain amount of power independently from their port number. The reference for these values are taken from Finisar data sheets that declare a consumption of 20 W for a single WSS module [22] (the module include some electronics, so the consumption of the WSS only is estimated to be one half of the module).

Three types of amplifier are defined: a low gain amplifier used to recover the signal attenuation in crossing the node modules (WSS, MSC, splitter and combiner), and two line amplifiers, one for amplifying the input signal in input (pre) and the other to launch the signal (booster) of the node. Power reference for these amplifiers are taken from Ciena public data [23] and from STRONGEST project [20].

Table 3-2: Formulas for power consumption computation of system boards

System Board	Power consumption computation formulas
ROADM line board	P_BCB+P_WSS+P_OAP+P_OAB+P_OPM+P_OSC
1x20 WSS A/D board	P_BCB+P_WSS
MxN WSS A/D board	P_BCB+P_WSS
Multicast switch board M x N	P_BCB+P_MSC+2xMxP_OAN
1x8 ASC board	P_PCB+2xP_OAN
1x16 ASC board	P_PCB+2xP_OAN
EDFA line board	P_BCB+2xP_OAB+P_OPM+P_OSC

Using the power consumption of elementary functions of Table 3-1 in the formulas of Table 3-2, the power consumption of ROADM boards are derived as shown in Table 3-3. An estimation of the number of slots required for each board is also provided.

Table 3-3: Power consumption of ROADM equipment

System Board	Power Consumption (W)	Capacity/slots required
Controller board and Fans (32 slots)	200	32 (capacity)
Controller board and Fans (16 slots)	140	16 (capacity)
ROADM line board	120	3
1x20 WSS A/D board	50	2
MxN WSS A/D board	50	2
Multicast switch board M x N (M=4)	75	2
Multicast switch board M x N (M=8)	115	2
1x8 ASC board	40	1
1x16 ASC board	40	1
EDFA line board	110	2

Using the power model defined, two examples of ROADM configuration are presented in Table 3-4 and Table 3-5. Both examples include all the boards except the transponders that require additional rooms on the shelves and whose power model is discussed in subsection 3.2.2.

Table 3-4: Example of degrees 2 ROADM with 2 Colorless A/D modules (35 ports on each line side)

System Board	Items	Power (W)	Slots
Controller board and Fans (16 slots)	1	140	
ROADM line board	2	240	6
1x20 WSS A/D board	2	100	4
1x16 ASC board	2	80	2

Total power (W)	Required slots

560	12

Table 3-5: Example of degrees 6 ROADM with 6 Colorless A/D modules (20 ports on each line side), 2 A/D CD-less modules (35 ports each) and 1 A/D CDC-less MSC module (16 ports)

System Board	Items	Power	Slots
Controller board and Fans (32 slots)	1	200	
Controller board and Fans (16 slots)	1	140	
ROADM line board	6	720	18
1x20 WSS A/D board	6	300	12
MxN WSS A/D board (8x20)	2	100	4
Multicast switch board M x N (8x16)	1	115	2
1x16 ASC board	2	80	2

Total power (W)	Required slots
1655	38

It should be noted that the controller board is always duplicated for node management reliability reasons, but one of the two controller boards is in hot standby and in this state it is supposed to have negligible power consumption. Therefore, in Table 3-4 and Table 3-5 the controller boards are count up one time while there are two of them in each shelf.

A tentative scheme of board allocation on the shelves for these two ROADM examples is shown in Figure 3-6 and**Error! Reference source not found.**.

Figure 3-6: example of a possible allocation of the boards in a 16 slots shelf for the ROADM node of Table 3-4.

Figure 3-7: example of a possible allocation of the boards in a 16 and a 32 slots shelves for the ROADM node of Table 3 5

3.2.2 Configurable transponder

DISCUS configurable transponder high level architecture derives from the set of network service that are required (see deliverable D6.1):

- DP-BPSK single carrier (40 GE)
- DP-QPSK single carrier (100 GE)
- DP-16QAM single carrier (2x100 GE)
- DP-BPSK dual carrier (100 GE)
- DP-16QAM dual carrier (400 GE)
- DP-QPSK quadruple carrier (400 GE)

A maximum of four 32 Gbaud optical carriers are foreseen and therefore the line functions of the configurable transponder will be composed by 4 independent coherent transceivers operating at 32 Gbaud with 3 configurable modulation formats: DP-BPSK, DP-QPSK, and DP-16QAM. These functions will be grouped onto a unique kind of configurable line board.

Since many client options are foreseen, the client functions of the configurable transponder will be housed on a separate board with respect to the line functions. The following three kinds of client boards seem the most viable:

- 4x40 GE ports;
- 4x100 GE ports;
- 2x400 GE ports (not yet standardized).

These client boards will be selected by the network designer based on the kind of client signals required in each network node. A client boards is connected with the associated line board through the shelf backplane.

The power consumption of the transponder boards are based on information available about current devices. Main references used to derive the power consumption parameters are Fujitsu [21] and Civcom [24].

A state of the art of 100 G transponder card is depicted in Figure 3-8 where the transition between the current and next generation is shown. The card is composed of a MSA (Multi-Source Agreement) module that include the network side optics and a transceiver (CFP) that is the client side optics.

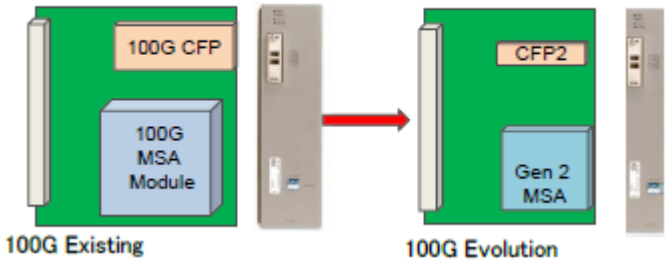

Figure 3-8: architecture of the 100 G card, current and next version expected in 2014

In Figure 3-9 the evolution in size and power consumption are also reported. It results that today a transponder consumes about 100 W (this is the case of Civcom device [24]) while in next generation with MSA Gen 2 module and CFP4 transceiver the power consumption should decrease under 50 W and 5 W respectively ([21]). The proposed power consumption for the DISCUS model are given in Table 3-6.

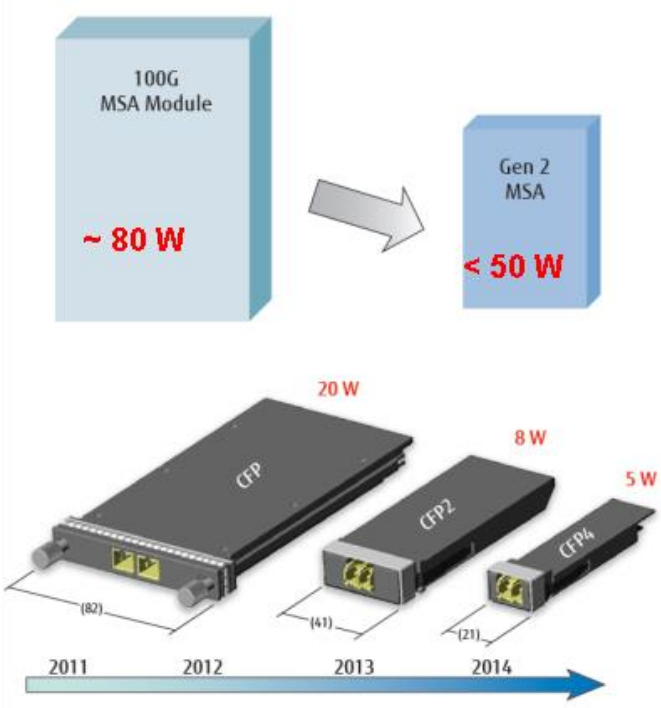

Figure 3-9: Evolution in size and power consumption of 100 Gbit/s transponder subparts (source Fujitsu [21])

Table 3-6: Power consumption of configurable transponders

System Board	Power Consumption (W)
4 carriers Line board	200
4x40 GE client board	116
4x100 GE client board	270
2x400 GE client board	TBD

3.3 Core Network Packet transport Layer

In this paragraph, a MPLS-TP core switch functional model is presented together with the related power consumption model.

The most advanced architecture of today's packet based switches is based on service cards and switching matrix as shown in Figure 3-10.

Figure 3-10: architecture of the DISCUS MPLS-TP core switch.

Service cards play the role of both line and client interfaces since in electronic packet switches the two functionalities are physically equivalent (i.e. service cards have grey optical interfaces that can be connected either to DWDM transponders, or to client equipment). The only exception is the case of coloured line interfaces where line interfaces encompass DWDM functionalities and are optically connected to ROADM A/D ports.

The switching functionalities of state of the art equipment are distributed onto many fabric cards as shown in Figure 3-10, in a redundant configuration. This means that the equipment can provide its full switching capacity even if one fabric card is out of service.

Based on these architectural trends and on the state of the art technology, the main characteristics of the DISCUS MPLS-TP switch can be envisaged as follows:

- 4 Fabric cards in 3+1 redundant configuration;
- 3.2 Tbit/s full duplex switching capacity;
- 16 service cards slots, with 200 Gbit/s capacity per slot.

Based on these characteristics, it is reasonable to define a set of client boards and line boards that exploit the whole 200 Gbit/s of each slot. The choice is then straightforward:

- Client boards:
  - 5x40GE (grey interfaces)
  - 2x100GE (grey interfaces)
- Line boards:
  - 5x40GE, 2x100GE (grey interfaces)
  - 32 Gbaud DP-QPSK dual carrier (2x100G)
  - 32 Gbaud DP-16QAM single carrier (200G)

The last two line boards are coloured line interfaces tailored for an electronic packet switch with 200 Gbit/s slot capacity. They represent a viable alternative to the four carriers, configurable line interface described in paragraph 3.2.2 when full exploitation of equipment slots capacity is required.

The equipment model described above reflects a state of the art of most advanced MPLS-TP switch but it do not reflect exactly any commercial piece of equipment. In fact most of the commercial equipment today rely on 100 Gbit/s service cards, even if in few cases 200 Gbit/s cards are declared ready. In addition, coloured cards as the one described in the model are in road map of the manufacturers but in our knowledge not yet ready (especially the single 200 Gbit/s single carrier DP-16QAM).

The method used to assign the power consumption to the equipment subparts was to collect power consumption data from a number of manufacturers (data are confidential and cannot be shown in the deliverable) and use them to infer the power consumption of a specific item of the model. In most cases the power consumption is known only for the whole equipment in a given configuration without the details about the partitioning between the subparts. For this reason, the model has been tuned by first assigning tentative values to the parameters and then by checking that the whole consumption of the piece of equipment were close into to the real data.

Another source for the parameter values setting for the DISCUS energy model was the STRONGEST project and in particular deliverable D2.4 [20], where values of power consumption for Carrier Ethernet equipment was reported. It was stated that the MPLS-TP equipment should have similar power consumption values (or, at least, not higher) compared to Carrier Ethernet ones. In the STRONGEST model the consumption is expressed in Watt per port, with port rates from 1 Gbit/s to 1 Tbit/s according to the Ethernet hierarchy. Consumption parameters for 100 Gbit/s and higher are predicted as those ports were not yet commercially available at the time the document was delivered (2012).

In general, it results that today equipment (a base of a sample of about ten different nodes is used) fully equipped with an assortment of 10 Gbit/s and 100 Gbit/s interfaces shows a specific power consumption in the range from 1500 to 3000 W/(Tbit/s) with an average of 2400 W/(Tbit/s).

Considering the STRONGEST project results in Table 3 of [20] each grey port at 100 Gbit/s (including the common parts overhead) is predicted to consume 205 W. It follows that the specific consumption of an equipment no matter how many ports is 1050 W/(Tbit/s).

Taking into account the above mentioned sources and that the equipment DISCUS is considering should be ready in short term future, we assume as reasonable specific power consumption for MPLS-TP fully equipped node with gray interfaces the minimum value of that parameter of today equipment, that is 1500 W/(Tbit/s). This values is about 37% less than the average value of the known commercial equipment.

Table 3-7 report the power parameter values for the MPLS-TP node. The model for the service cards of 200 Gbit/s takes into account a common part that require 200 W for the Processing card and the interfaces modules (grey transceivers or coloured WDM modules) that require their own power consumptions. For the consumption of grey transceivers the next generation CFP4 is taken as a reference (see [21]).

Table 3-7: Power consumption parameters of MPLS-TP equipment

Component	Power (W)	Notes
Controller board and Fans	200	For Fabric board and up to 16 Service Boards
Fabric board (3,2 Tbit/s)	1000	4 cards, 3+1 redundant
5x40GE board	220	200 W plus 5 x 40GE grey transc. 4 W each
2x100GE board	210	200 W plus 2 x 100GE grey transc.5 W each
DP-QPSK dual carrier board	400	200 W plus 2 x DP-QPSK 100 Gbit/s WDM tun.
DP-16QAM single carrier board	320	200 W plus 1 x DP-16QAM 200 Gbit/s WDM tun.

Assuming the parameter values reported in Table 3-7 an example of two fully equipped nodes are given in Table 3-8 . Configuration A is provided of grey interface for both client and network lines while configuration B includes grey interfaces for clients and WDM coloured interfaces for network lines.

Table 3-8: Example of MPLS-TP node configurations and related power consumptions

		Config. A (grey itf. only)		Config. B (grey and coloured itf.)	
	PC (W)	Units	Power (W)	Units	Power (W)
Ctrl brd & Fans	200	1	200	1	200
Fabric brd	1000	1	1000	1	1000
5x40GE brd	230	8	1760	2	440
2x100GE brd	216	8	1680	4	840
DP-QPSK DC brd	400	0	0	6	2400
DP-16QAM SC brd	320	0	0	4	1280

	Config. A	Config. B
Total Power (W)	4640	6160
Specific Pow. Cons. (W/Tbs)	1450	1925

Multishelf node for capacity greater than 3.2Tbit/s.

For node capacities higher than 3.2 Tbit/s, a multi-shelf node made up of multiple single shelf equipment interconnected together can be assumed. In first

approximation for the common parts the power consumption of nodes requiring more than 3.2 Tbit/s of switching capacity can be evaluated as an integer multiple of the consumption of basic 3.2 Tbit/s node (Controller, Fan, Fabric). The service boards power consumption component is evaluated as in the single shelf node, summing up the consumptions of installed boards.

3.4 Power consumption modelling at network level

Beside telecommunication equipment, additional power consumptions sources in central offices must be considered. The main ones are the following:

- equipment rooms cooling;
- DC power supply;
- equipment rooms lighting.

Among these additional power consumptions sources the most important one is the equipment room cooling that, in Telecom Italia experience, may account for as much as 22% of the total central office power consumption. This percentage varies in function of the specific cooling technologies and the climatic conditions. Based on Telecom Italia recent data, DC power supply and lighting altogether may account for approximately 15% of central office power consumption. For DISCUS network evaluation purposes these figures will be regarded as tentative values unless a further analysis will be available in literature.

Therefore, to calculate the overall power consumption of the DISCUS central offices, the equipment power consumption calculated by the previous models will be multiplied by a 100/(100-37)=1.587 factor.

3.5 Summary/Conclusions

In this Chapter we have derived the power consumption models of the Photonic and Packet Transport equipment of the DISCUS core network.

For the Photonic equipment, we have first identified the optical functionalities required in ROADM nodes and configurable transponders and then we have grouped these functionalities into network system boards. The typical power consumption of such boards have been evaluated based on data available in literature and information obtained from the IDEALIST project.

As far as it regards the Packet Transport equipment, i.e. the MPLS-TP packet switch, we have considered the most advanced architecture of electronic packet switches and we have envisaged a set of line, client and switching boards that fulfil the DISCUS service requirements. The power consumption of these boards have been evaluated based on data available in literature.

Additional power consumption sources like DC power supply and central office cooling and lighting have been modelled as well.

These models can be used to evaluate the core network power consumption in function of the actual traffic as soon as the traffic matrix and related equipment configuration will be shaped.

4 Power Consumption and Resilient Studies

4.1 Introduction

Survivability to device failures is a fundamental requirement in WDM core networks. Survivability is achieved by installing/reserving redundant (protection) resources, which will be used only in the case of a failure to restore the affected connections. Such resources, on the other hand, are typically maintained active, independently of the failure pattern, and thus consume power even when unutilized, i.e., they are not used in an energy efficient way.

Energy saving is gaining importance in wavelength division multiplexing (WDM) networks as a way to reduce the capital expenditures of network operators. Strategies for reducing the power drained by the optical layer of survivable WDM networks mainly resort to techniques that turn off unused devices. These techniques can be enabled by the introduction of a sleep mode option in the equipment. Since the devices deployed for protection are unused most of the time (e.g. in absence of failures), they can be set to sleep and promptly re-activated when the recovery is triggered. However performing these operations while at the same making sure that the other network parameters (e.g. cost, blocking ratio) are not affected, requires careful design and/or provisioning operations.

Despite the high number of recent publications targeting green telecommunication networks, only a limited number of studies focus on energy efficiency in the context of optical network resiliency. Sleep mode for protection was proposed in [25][27] and is able to save significant amount of power especially at low loads, when the planning [25][28] and the dynamic management [29] of survivable WDM networks with path protection is properly optimized. The path protection technique concerns the possibility to share protection resources among different connections, i.e., by using the shared path protection (SPP) mechanism. Energy-efficient planning of static networks with SPP has been addressed in [30][31]. Both techniques (i.e., sleep mode and SPP) can been exploited together[32][33] for enhanced power saving.

This section focuses on a number of tradeoffs that are crucial while studying reliable and energy efficient WDM networks. The first trade off to be considered is between the level of energy savings vs. the amount of wavelength resources needed when an SPP-based WDM network design is performed. A similar tradeoff is assessed in the case of dynamic provisioning of optical connections, where in this case energy savings performance is weighted against the networks blocking ratio. Finally the last tradeoff to be studied is about the impact that energy efficient provisioning strategies have on the reliability level of the network components.

4.2 Energy and cost efficient WDM design with Shared Path Protection

Energy-efficient routing strategies tend to group connections together on a subset of the network links in order to put lightly loaded resources into sleep mode. However, in this way the vulnerability to failures increases (i.e. one failed “packed”

link leads to the possible disruption of a higher number of connections). On the other hand, survivable routing strategies aim at spreading the provisioned connections over different resources, thus limiting the possibility to put to sleep mode lightly loaded network links. For example, with SPP a high shareability of protection resources translates into low energy saving performance, and vice versa. To address this trade-off energy-aware survivable routing strategies are needed. This problem has been partially addressed in [30] where an ILP model for energy-efficient shared backup protection is proposed with the objective of minimizing both capital and operational expenditures while letting those fiber links associated only with backup paths to be put in sleep mode. However, since the problem is NP-complete, ILP solutions are not scalable for larger problem sizes. Therefore, this section presents a heuristic for the energy-aware SPP (EASPP) design problem based on the use of a separate auxiliary graphs for primary and backup path routing to encourage both shareability and energy-efficiency. The details of the heuristic are available in [31] and are briefly presented next.

4.2.1 Energy-Aware Shared Path Protection (EASPP) heuristic

An energy-efficient heuristic for shared path protection (EASPP) is presented in this section to minimize both capacity and power consumption (see Algorithm 1). The latter is achieved by trying to concentrate as much as possible (i.e. pack) wavelength paths into fiber links. This in turns allows for putting unused fiber resources into low power/sleep mode. Capacity is on the other hand minimized the by encouraging shareability among backup paths.

Given: The physical topology consisting of the set of nodes and links with geographical distances as the link weights *G(V,E)*, the set of lightpath requests *D[i]*, the maximum number of wavelengths supported on each link (*W*), and the power consumption values for amplifiers and optical switches derived from [26].

Find: A shared-path-protected primary/backup path-pair, i.e., (*P*,*B*) for each request; total power consumption.

Objective: Minimize both capacity and power consumption to address survivability and energy-efficiency trade-off.

Stages	**Steps**	**Actions**
(1) Initial routing	1. 2.	**for** each $i \in D$ Find *Path[i]*: Dijkstra(i,G_D) **end for** Sort *D[i]* according to increasing distance along *path[i]*
(2) Primary path routing	3. 4. 5.	**for** each $i \in D$ Update link weights on G_E(V,E) according to (Table 4-1(a)) *K* = Find k-shortest-path(i,k,G_E) ***P*** = Path with the shortest distance (*K*)
(3) Backup path routing	6. 7.	Update link weights on G_D(V,E) according to (Table 4-1(b)) ***B*** = Dijkstra(i,G_D) **end for**

Algorithm 1: EASPP (Energy-Aware Shared Path Protection)

As shown in Algorithm 1, EASPP has three stages. In the first stage all lightpath requests in *D[i]* are sorted based on the ascending value of the total distance of their routes, i.e., from the shortest to the longest, according to the information in *path[i]* (candidate paths vector). The second and the third stage are in charge of primary and backup paths routing, respectively, using the link cost assignments presented in Table 4-1. In Stage 3 the link weights of the primary paths are updated. In Step 4 and 5, *k* paths with the least power consumption are found (i.e. by running the Yen's algorithm [34] on G_E(step 4) and in order to minimize the capacity consumption, the one with the shortest distance is selected as the primary path, i.e., *P* (step 5). Finally the backup path, i.e. *B*, is routed in steps 6 and 7.

4.2.2 Primary and backup routing scheme

Table 4-1 presents the penalty weight assignments for (a) primary and (b) backup paths routing. The notation is the following: C_e: weight of link *e*; d_e: distance of link *e*; a_e: power consumption of amplifiers on link *e*; f_e: number of free wavelengths on link *e*; B_e: number of wavelengths in the backup pool where shared wavelengths are reserved on link *e*; $v_e^{e'}$: number of backup wavelengths reserved on link *e* to protect primary paths passing through link *e'*; *M*: amplifier power consumption of the longest path, E_S: optical wavelength converters and the switching power consumption per wavelength, *T*: packing parameter.

Table 4-1: Penalty weight assignments for (a) primary and (b) backup paths routing

Type of routing		Weight values	Cases
(a)	C_e for **primary path** routing for $G_E(V,E)$	∞; $T \times E_S$ M; $E_S + a_e$;	(I) $f_e=0$ (II) if $e \in P$ (III) if $e \in (B \setminus P)$ (IV) if $e \notin (P \cup B)$
(b)	C_e for **backup path** routing for $G_D(V,E)$	∞; d_e; $\varepsilon \times d_e$ $\varepsilon \times 5d_e$ $\varepsilon \times 10d_e$;	(I) if $e \in P$ or if ($f_e=0 \wedge \exists\, e' \in P$: $v_e^{e'}=B_e$) (II) if $e \in P \wedge$ backup W not shareable (III) if $e \in B \wedge$ backup W shareable (IV) if $e \in (B \setminus P) \wedge$ backup W not shareable (V) if $e \notin (P \cup B)$

Primary path routing uses the auxiliary graph $G_E(V,E)$ defined in Table 4-1(a). Link weights are assigned to G_E considering the additional power consumption in case the request chooses the candidate link. In Table 4-1(a) (I) corresponds to, insufficient resources, and (II) defines the weights for the links used by primary paths. Since the optical switching power E_S is a relatively small value this weight assignment encourages primary paths to pack. Therefore in order to tune this packing behavior we used a packing parameter *T* for case (II). With a small value of *T*, more packing is encouraged, hence energy minimization. In case (III), links utilized by only backup paths are assigned a big cost (*M*) representing the maximum power consumption of the amplifiers along the longest path, in order to separate backup routes from primary. Case (IV) defines the additional power consumption when a link is turned on and used for the first time.

Backup path routing uses the auxiliary graph G_D, whose weights are based on distances and encourages shareability as shown in Table 4-1(b). Case (I) corresponds to insufficient resources, and (II) represents the case when a primary

path uses a link and backup wavelengths on that link are not shareable. In this case a penalty is applied, as we need to leave room for primary paths to be packed. In case (III), in order to encourage shareability, the smallest cost is assigned to the links accommodating backup paths with shareable wavelengths. Here, a link vector technique [36] is used to track the shareability information of the links. In case (IV), in order to separate primary and backup paths as much as possible, a second priority is given to the links used by only backup paths although the wavelengths are not shareable. Case (V) represents unutilized links, which are encouraged to be used only as a last priority.

4.2.3 Numerical Results

For performance evaluation, EASPP is compared with a conventional energy-unaware SPP (EUSPP) approach, i.e., where capacity consumption is minimized. In order to evaluate the effect of sleep mode on SPP, power consumption in EUSPP is calculated for two cases: EUSPP-S where backup resources are in sleep mode and EUSPP-NS with backup resources being active. For a fair comparison, EUSPP follows a two-step approach by routing primary paths on G, the distance weighted graph and backup paths on a simplified version of G_D. In Table 4-1(b), instead of cases (II)-(IV) just shareable and non-shareable cases are taken into account which ensure shareability by using the same cost function applied in case (II). Moreover, performance of EASPP is compared with the optimum solutions from an ILP design [30] with 20 connection requests (Table 4-2).

	ILP (min cap.)	**ILP (min en.)**	**EASPP (T=20)**	**EASPP (T=1)**
Total power	1871.003	792.524	1313.196	1001.361
Primary W	32.6	82	38.6	55
Backup W	16.8	30.4	31.6	36.2

Table 4-2: Comparison of ILP results (minimum capacity and minimum energy) with EASPP (T=20 and T=1) for total power consumption and primary and backup wavelength usage with 20 connection requests.

The network topology used in this study is the Cost 239 European Network [37] with 11 nodes and 26 bidirectional links with link distances from 180 to 1000km. Each link supports W=16 wavelengths. Connection requests are generated according to uniform distribution among source and destination nodes. Each request requires the bandwidth of a full wavelength channel operating at 10Gbps. Power consumption parameters are set according to [38] as follows: optical wavelength converters and switching per wavelength consumes a total E_S= 1.757 W. Power consumed by in-line amplifiers is calculated by the formula $a_e = E_a \times A_e$ where E_a=9 W (power consumption of an in-line amplifier) and $A_e = \lfloor d_e / 80km \rfloor$ +2 (number of in-line amplifiers on link e). Total power = $E_S p + \sum_e a_e l_e$ where p denotes the number wavelength links used by primary paths and l_e =1 if link e is used by primary paths. In EASPP T=20 and M=306. The results in Figure 4-1 are obtained with T=20 which gives the best capacity and power consumption among the tested values. In order to show the impact of tuning parameter, we demonstrated the results for both T=1 and T=20 in Table 4-2.

Table 4-2 compares EASPP with the upper and lower bounds, i.e., the two ILPs where (1) capacity consumption is minimized and (2) power consumption is minimized. EASPP overcomes the capacity consumption drawback of the optimum energy case, and at the same time still has significant savings in power consumption. EASPP (T=20) saves up to 53% of wavelength-links used by primary paths compared to minimum-energy ILP and up to 30% reduction of power consumption compared to minimum-capacity ILP. When the packing parameter T is tuned to 1, the energy saving increases to 46% while the capacity consumption gain decreases to 33%.

Figure 4-1(a) compares EASPP with conventional EUSPP-S and EUSPP-NS with respect to total power consumption in watts. EASPP outperforms EUSPP except for larger number of connection requests where it behaves very close to EUSPP-S. The reason is that with high number of connection requests (i.e. at high load) all resources need to be utilized, which reduces flexibility in packing primary paths, hence the sleep mode option cannot be enabled and there will be no gain in terms of power consumption. By taking into consideration energy-efficiency in the routing phase, EASPP performs much better than energy unaware approaches even at the moderate traffic load, and saves up to 30% and 52% power compared to EUSPP-S and EUSPP-NS respectively.

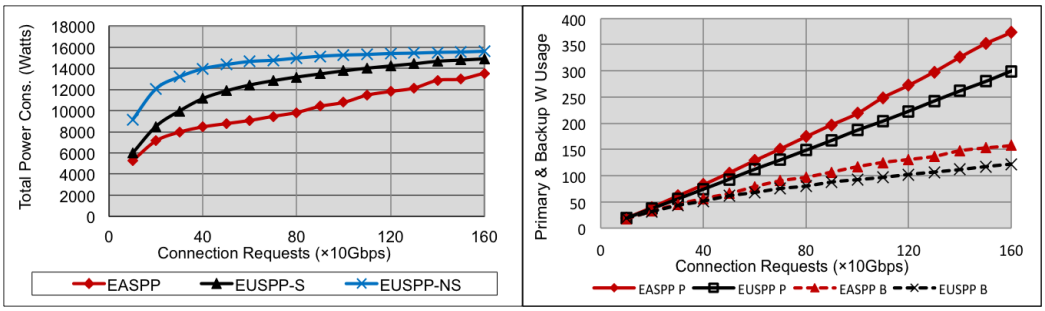

(a) (b)

Figure 4-1: Total power consumption vs. connection requests (a) and P and B wavelength links vs. connection requests (b).

Figure 4-1(b) shows the wavelength-link usage by primary and backup paths as a function of number of connection requests in both the energy-aware and unaware approaches. In order to gain in power consumption, we need to trade capacity consumption. EASPP packs primary paths as much as possible, which can lead to taking longer paths. In order to gain in energy, EASPP trades up to 20% and 24% of primary and backup wavelength usage over EUSPP.

4.3 Energy efficient WDM Shared Path Protection provisioning with reliability differentiation

When applying energy-saving techniques in dynamic SPP-based WDM networks, the drawback is a possible degradation of the network performance in terms of blocking probability [39]. This is due to the fact that the minimization of power consumption and the maximization of resource utilization are conflicting objectives. For instance, the routing of the protection path for a lightpath may span

on a large number of links, which are shared and used only for protection, leading to a low power consumption but to a poor resource utilization in the long run.

To overcome this issue, it is possible to consider the concept of *Differentiated Reliability* (DiR) [40], which enables connections to have different reliability levels. In DiR the protection path need not be always available for any possible link failure scenario, resulting in a significant reduction of the resource utilization and thus the blocking probability [41]. However, the impact of DiR on the power consumption of the network is still unclear. Initial finding [42] indicates that power saving up to about 20% are achievable when a static WDM network is planned in an energy-efficient way with DiR support compared to the conventional dedicated path-protection scheme. It would be interesting to see if a similar energy saving performance is achievable also in the case of dynamic provisioning and with SPP.

Towards this end this section will introduce a heuristic called Energy-Aware SPP-Based DiR (EASPP-DiR) that applies the DiR concept to a dynamic and reliable WDM network with the objective of jointly optimizing energy efficiency, resource utilization, and offered reliability performance beyond the requested level (referred to as reliability excess). The details of the heuristic are available in [43] and are briefly presented next.

4.3.1 Energy-Aware SPP-Based DiR (EASPP-DiR)

The Energy-Aware SPP-DiR algorithm aims at finding for each demand *d* a pair of working and protection paths ($w^{(d)}$,$b^{(d)}$) able to satisfy the wavelength continuity constraint and the $MCFP^{(d)}$ requirement, while keeping both the number of used resources and the energy consumption at a minimum. The MCFP (Maximum Conditional Failure Probability) level represents the maximum acceptable probability that, upon a link failure, the connection will not survive [40][41][43]. Let $\lambda_w^{(d)}$, $\lambda_b^{(d)} \in \Lambda$ (i.e., the wavelength set) be the wavelengths that are chosen for the working and protection paths of *d*, respectively. Let $H_w^{(d)}$ be the set of links that are in the working path of *d*. Let $H_b^{(d)}$ be the set of links that are in the protection path assigned to *d*. Let $H_u^{(d)} \subseteq H_w^{(d)}$ be the set of working links of *d* that are unprotected, i.e., upon the failure of a link in $H_u^{(d)}$ demand *d* is permanently disrupted. Let $MCFP^{(d)}$ be the minimum reliability degree requested by *d*. Let *D* be the set of demands that are already established in the network. Let $\hat{d}$ be an arriving demand. $\hat{d}$ is accepted and inserted in *D* if all the following constraints are satisfied:

- *link-disjointness*: i.e., the working and the protection path must be link-disjoint, i.e.,

$$H_w^{(\hat{d})} \cap H_b^{(\hat{d})} = \{\varnothing\} \tag{4.1}$$

- *protection sharing*: a protection wavelength cannot be shared by multiple demands if they share the same (protected) working link, i.e.,

$$\forall d \in D, d \neq \hat{d}: \begin{cases} (H_w^{(d)} \setminus H_u^{(d)}) \cap (H_w^{(\hat{d})} \setminus H_u^{(\hat{d})}) \neq \{\varnothing\} \\ H_b^{(d)} \cap H_w^{(\hat{d})} = \{\varnothing\} \vee \lambda_b^{(d)} \neq \lambda_b^{(\hat{d})} \end{cases} \quad (4.2)$$

- *MCFP requirement*: the conditional failure probability guaranteed to demand $\hat{d}$ does not exceed the $MCFP^{(\hat{d})}$ required by $\hat{d}$, i.e.,

$$P_f^{(\hat{d})} = \sum_{(m,n) \in H_u^{(\hat{d})}} P_f(m,n) \leq MCFP^{(\hat{d})} \quad (4.3)$$

If any of the above constraints cannot be satisfied, demand $\hat{d}$ is blocked. Notice that the protection paths of demands $\hat{d}$ and $d \in D$ are allowed to share a wavelength, i.e., $\lambda_b^{\hat{d}} = \lambda_b^d$, only if the following constraint is satisfied:

$$(H_w^{(\hat{d})} \cap H_w^{(d)}) \subseteq (H_u^{(\hat{d})} \cap H_u^{(d)}) \quad (4.4)$$

The selection of the routing and wavelength for $\hat{d}$ (i.e. $w_i^{(\hat{d})}$, $b_j^{(\hat{d})}$ and $\lambda_{b_j}^{(\hat{d})}$ is jointly optimized for the number of resources used, the power consumption, and the excess of reliability. The cost function, $C_{i,j,k}^{(\hat{d})}$, is a linear combination of these three quantities weighted with coefficient g for the resource cost, coefficient h for the power consumption, and a unitary coefficient for the excess of reliability:

$$C_{i,j,k}^{(\hat{d})} = \gamma \cdot \left(\left| H_{w_i}^{(\hat{d})} \right| + \left| H_{b_i}^{(\hat{d})} \right| - \left| H_{s_{(i,j,k)}}^{(\hat{d})} \right| \right) + \eta \cdot \left(P_{w_i} + P_{b_{(i,k)}} \right) + \left(MCFP^{(\hat{d})} - P_{f_{(i,j,k)}}^{(\hat{d})} \right) \quad (4.5)$$

The first term in (eqn. 4.5) gives an estimation of the resources (that is number of links on which wavelengths are to be reserved) needed to provision $\hat{d}$ on $w_i^{(\hat{d})}$ and $b_j^{(\hat{d})}$ using wavelength $\lambda_{b_j}^{(\hat{d})} = \lambda_k$ for $b_j^{(\hat{d})}$. Shared resources are accounted by subtracting the number of protection links in which the protection wavelength is shared, i.e., $\left| H_s^{(\hat{d})} \right|$, with $H_s^{(\hat{d})} \subseteq H_b^{(\hat{d})}$. The second term accounts for both the power consumption of $w_i^{(\hat{d})}$ and $b_j^{(\hat{d})}$, i.e., P_{w_i} and P_{b_i} (see [43] for more details on the power model). Finally, the third term includes the excess of reliability defined as the difference between the required $MCFP^{(\hat{d})}$ level and the value of $P_{f_{(i,j,k)}}^{(\hat{d})}$ computed as in (eqn. 4.3) for the specific triplet $w_i^{(\hat{d})}$, $b_j^{(\hat{d})}$, and $\lambda_{b_j}^{(\hat{d})}$.

Algorithm 2 aims at computing the routing of both the working and the protection paths, and at selecting the protection resources for each arriving demand $\hat{d}$. The route of the working path (i.e. $w_i^{(\hat{d})}$) is selected within a set of pre-computed candidates $W^{(\hat{d})}$. For path $w^{(\hat{d})}$, the route of the protection path (i.e., $b^{(\hat{d})}$) is selected among a number of pre-computed candidates $B^{(\hat{d})}$. First, the algorithm checks the wavelength availability for the working path by starting from the first path in $W^{(\hat{d})}$, $w_1^{(\hat{d})}$. If the same wavelength is not available on all the links of $w_1^{(\hat{d})}$, the path is discarded and the next path in $W^{(\hat{d})}$ is considered. Otherwise a link-

disjoint protection paths in $B^{(\hat{d})}$ is considered (i.e., satisfying the link disjoint constraint in (eqn. 4.1)).

$\mathcal{G}(\mathcal{V}, \mathcal{E})$: network topology;
$\hat{d}$: lightpath demand;
$W^{(\hat{d})}$: set working paths for $\hat{d}$ sorted for hop length;
$B^{(\hat{d})}$: set protection paths for $\hat{d}$ sorted for hop length for path $w_i^{(\hat{d})}$;
Initialization: $\widetilde{C} = -1$;
for each path $w_i^{(\hat{d})} \in W^{(\hat{d})}$ **do**
  Let $\Lambda_{w_i}^{(\hat{d})}$ be set of continuous wavelengths for $w_i^{(\hat{d})}$;
  if $\Lambda_{w_i}^{(\hat{d})} \neq \emptyset$ **then**
    for each $b_j^{(\hat{d})} \in B^{(\hat{d})}$: $H_w^{(\hat{d})} \cap H_b^{(\hat{d})} = \{\emptyset\}$ (Eq. (1)) **do**
      Let $\Lambda_{b_i}^{(\hat{d})}$ be the set of continuous wavelengths for $b_j^{(\hat{d})}$;
      if $\Lambda_{b_i}^{(\hat{d})} \neq \{\emptyset\}$ **then**
        for each $\lambda_k \in \Lambda_{b_i}^{(\hat{d})}$ **do**
          if $w_i^{(\hat{d})}, b_j^{(\hat{d})}, \lambda_k$ satisfy Eqs. (2) and (3) **then**
            Compute cost $C_{i,j,k}^{(\hat{d})}$ (Eq. (5));
          end if
        end for
      end if
    end for
  end if
end for
Select $w_i^{(\hat{d})}$, $b_j^{(\hat{d})}$ and λ_k : $\widetilde{C} = \min_{i,j,k}\{C_{i,j,k}^{(\hat{d})}\}$;
if $\widetilde{C} \neq -1$ **then**
  Return $w_i^{(\hat{d})}$, $b_j^{(\hat{d})}$, λ_k, $\Lambda_{w_i}^{(\hat{d})}$;
else
  Block $\hat{d}$;
end if

Algorithm 2: EASPP (Energy-Aware Shared Path Protection)

For each link-disjoint path in $B^{(\hat{d})}$, $b_j^{(\hat{d})}$, the resource availability is checked. First the set of available continuous wavelengths $\Lambda_{b_i}^{(\hat{d})}$ is computed, then each $\lambda_k \in \Lambda_{b_i}^{(\hat{d})}$ is checked. If λ_k is already used for protection purposes by other protection paths the protection sharing constraint (eqn. 4-2) is checked. If satisfied and if the MCFP requirement (eqn. 4.3) is met, then the triplet w_i, b_j, and λ_k is a feasible solution and the value of $C_{i,j,k}^{(\hat{d})}$ is computed (eqn. 4.5). Among all the feasible solutions, the one at minimum cost $C_{i,j,k}^{(\hat{d})}$ is selected. If a feasible solution is not found, then $\hat{d}$ is blocked. Finally, the wavelength for the working path $\lambda_w^{(\hat{d})}$ is selected within the set of available wavelengths $\Lambda_{w_i}^{(\hat{d})}$ using the first-fit strategy.

4.3.2 Numerical results

The performance of the EASPP-DiR algorithm is assessed with a custom-built event-driven simulator. The WDM network is modeled as a graph *G(V,E)*, where *V*

represents the set of nodes and E the set of unidirectional links. The evaluation is carried out on the Pan-European topology (COST 239) [37], which consists of 11 nodes and 52 unidirectional links, with 16 wavelengths per link. The link failure probability is derived using a uniform distribution of failures, i.e., $P_f(m,n) = \frac{1}{52}$" (m,n)Î E. Demands are assumed to arrive in the network following a Poisson process. Established lightpaths are assumed to have an exponentially distributed duration, whose average value is set to 1. Demands are uniformly distributed among all node pairs. Unless otherwise specified, each demand is assigned the same reliability requirement $MCFP = MCFP^{(d)} = 0.02$. With this value and in the network topology under consideration, each demand may be able to have up one working link that is unprotected, i.e., $\left|H_u^d\right| = 1$," d at most. The number of candidate routes for each working path and for each protection path is set to 5, which are computed using K shortest path routing [44].

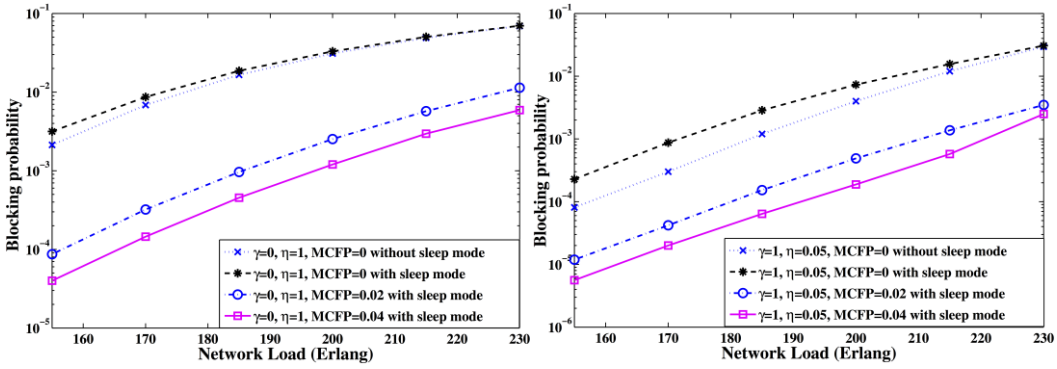

(a) (b)

Figure 4-2: Blocking probability versus offered network load when minimizing power consumption (a), and Blocking probability versus offered network load when minimizing power consumption and then resource utilization (b).

In Figure 4-2(a), the cost function is tuned for minimizing the power consumption, i.e., $g = 0, h = 1$.The impact of the MCFP level and sleep mode is assessed. Two insights can be gained. First, the blocking probability slightly increased when sleep mode is enabled. The reason is that, for the working lightpaths, in the presence of sleep mode the cost function forces the selection of longer paths (i.e., to set as much as possible resources in sleep mode) rather than shorter ones but without sleeping links. In turn, this leads to a higher resource utilization and thus higher blocking. Second, an improvement of more than one order of magnitude in blocking probability can be achieved when a lower reliability level is requested, i.e., *MCFP*=0.02. However, if the reliability level is further decreased (e.g., *MCFP=0.04*), the marginal improvement reduces.Figure 4-2(b) shows the value of the blocking probability when the cost function aims at minimizing the power consumption as primary objective and the resource utilization as a secondary objective. By accounting also for the resource utilization, the blocking probability is reduced by more than one order of magnitude with respect to the results for power optimization only, i.e., Figure 4-2(a), for all the different scenarios.

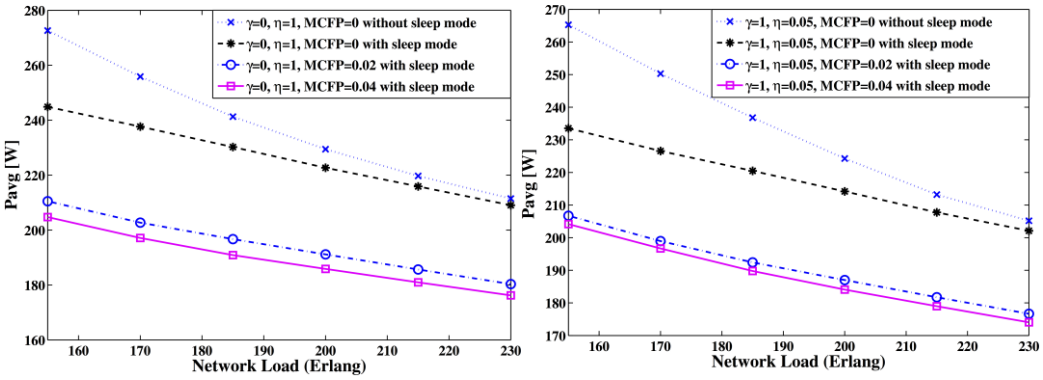

(a) (b)

Figure 4-3: Avg. power per established lightpath versus offered network load when minimizing the power consumption (a), and Avg. power per established lightpath versus offered network load when minimizing the power consumption and then the resource utilization (b).

In Figure 4-3(a), the cost function is tuned for minimizing the power consumption. The power consumption per lightpath decreases with the offered network load. The main reason is that the power consumption of load-independent devices (e.g., power consumption of in-line amplifiers, which can be considered independent of the number of amplified working lightpaths) can be shared among a larger number of lightpaths. By introducing the sleep mode, the slope of the curve is reduced, meaning that less power is wasted at low loads for powering scarcely used resources. This results in a power saving of about 10% at low loads. By closely matching the connection reliability level (*MCFP*=0.02), the power saving can be further improved by 13%. However, there is no significant advantage in further increasing MCFP (e.g., *MCFP*=0.04). This limitation is mainly due to the network topology, which is highly connected. Indeed the network connectivity leads to paths with short hop lengths, making it difficult to find protection paths in which more than one link can be unprotected. Figure 4-3(b) shows the average power consumption per lightpath when the cost function aims at minimizing the power consumption as primary objective and the resource utilization as secondary objective. The curves experience the same trend as in Figure 4-3(a). However, by incorporating the resource cost factor in the optimization function, the power consumption reduces compared to Figure 4-3(a). This unexpected result can be explained by the fact that among the different solutions at minimum power the one using less resource is selected.

4.4 Impact of energy efficient strategies on the lifetime of core components

As we have already seen so far most of the green approaches in core WDM networks are based on the concept that network components that are not used are either switched off or put into sleep mode [45]. However, frequent transitions between operational and sleep/off conditions may negatively impact the component reliability performance [46]. For example, cyclic temperature changes cause faster deterioration of solder connections [47][48], thus potentially reducing the circuit's lifetime. This possible reliability performance degradation may introduce additional operational expenditures (OPEX) in terms of failure reparation, which has to be taken into account in the overall OPEX calculation

when energy saving techniques are used. Therefore, a tradeoff between the energy (and consequently the cost) saved by a specific green strategy and the extra expenses deriving from a shorter lifetime of one or more network components need to be carefully assessed. This tradeoff can be measured in terms of *maximum allowable failure rate increase* where the extra reparation cost due to the additional failures would be covered by the saving obtained by a given green strategy. An assessment in this direction was done for optical access networks [45], where it was found that the frequent state transitions caused by a sleep-mode-based energy-efficient scheme may even increase the overall OPEX in the network. On the other hand, even though a number of green provisioning strategies have been proposed for optical core networks (e.g., [39][41][49]) none of them analyze the possible impact these strategies have on the network components' lifetime. A detailed study in this regard is presented in [50] and it is summarized next.

4.4.1 Maximum allowable failure rate increase: a component level assessment

This section presents an assessment of the maximum allowable failure rate increase of the main active components used in a WDM core network. The analysis is done by considering a number of potential energy saving thresholds, as a result of different energy saving profiles. The total operational expenditure $OPEX_T$ related to a given component is defined as the sum of energy consumption and reparation related costs and it is calculated based the following quantities:

- $OPEX_E$: the cost related to energy consumption;
- $\Delta OPEX_E$: the energy savings obtained by a low-power-mode operation;
- $OPEX_F$: the reparation cost in normal operating conditions;
- $\Delta OPEX_F$: the cost increase related to additional failure reparation(s) caused by the increased failure rate as a consequence of the transitions between low and high power modes.

Other operational expenses (e.g., floor space renting, building maintenance, service provisioning costs) are not considered because they do not change whether or not a low power mode is used. As a result $OPEX_T = OPEX_E - \Delta OPEX_E + OPEX_F + \Delta OPEX_F$. The $OPEX_E$ and $\Delta OPEX_E$ consider both the energy cost (USD/kWh) and the device energy consumption in active and sleep mode. The $OPEX_F$ and $\Delta OPEX_F$ take into account failure rate, failure rate variation, failure reparation cost (as a function of manpower cost), Mean Time To Repair (MTTR), and number of personnel required for reparation. The details of the OPEX models are presented in [46][51]. The respective OPEX and ΔOPEX costs are calculated on a per-year basis. We define the maximum allowable failure rate increase for a given component when energy related cost saving compensates the additional failure related cost, i.e., $\Delta OPEX_E = \Delta OPEX_F$.

Table 4-3 shows how the maximum allowable failure rate increase varies (in percent) as a function of a number of energy saving thresholds. Results are presented for different active network components. Passive components such as splitters, (de)multiplexers, and patch panels are not considered in this study because they are not the target of any energy saving mechanism. For each component the table also provides information about failure rate, MTTR, number

of personnel required for failure reparation (i.e. Pers.), and energy consumption, all under normal operation conditions. The failure rate is measured in FIT (Failure in Time), which corresponds to one failure during 109 hours. The energy price and the labor rate are assumed to be 0.27 USD/kWh and 190 USD/h, respectively [46].

Table 4-3: Maximum allowable failure rate increase as a function of possible energy savings.

Component	Failure rate [FIT]	MTTR [h]	Pers.	P [W]	Max. allowable failure rate increase with energy saving of:				
					10%	25%	50%	75%	95%
Transponder [51]	256	2	1	70	1895%	4737%	9475%	14213%	18004%
Regenerator [51]	256	2	1	70	1895%	4737%	9475%	14213%	18004%
Optical Switch [52]	5467	2	1	60	76.1%	190.1%	380.3%	570.5%	722.6%
ROADM [53]	3300	2	1	35	73.5%	183.8%	367.5%	551.3%	698.3%
EDFA [51]	2000	6	2	8	4.6%	11.6%	23.1%	34.7%	43.9%

As shown in Table 4-3, the maximum allowable failure rate increase of transponders/regenerators may vary between 1895% and 18004% (depending on the energy profile). For Reconfigurable Optical Add/Drop Multiplexers (ROADMs) and optical switches the maximum allowable failure rate increase is smaller than the one of transponders/regenerators, but still considerably high. As a result, it can be concluded that for these components the impact of frequent on/sleep transitions on the reliability performance is not a concern. In fact the extra reparation cost is easily compensated by the energy savings, i.e., $\Delta OPEX_E >> \Delta OPEX_F$.

However, for EDFAs the maximum allowable failure rate increase is relatively small, i.e., between 4.6% and 43.9%. Even when the energy savings might be potentially high (i.e., 95%) the maximum allowable failure rate increase is only 43.8%. As of today, there are no available data to assess the impact that on/off transitions have on the failure rate of currently deployed EDFAs. It is, on the other hand, possible to speculate around these values using data available for other electronic devices. After all, the underling physical phenomena responsible for the decrease of the reliability performance are similar (e.g., temperature variation causing strain creation in the solder [47][48]). The study in [54] shows that when a sleep-mode-based approach is applied to a System on Chip (SoC), the failure rate increases between 11% and 43% for energy savings levels between 50% and 90%, respectively. If a similar reliability performance decrease is assumed for EDFAs then, based on the results in Table 4-3, there might be instances in which using energy saving strategies may not be beneficial anymore, i.e., $\Delta OPEX_E < \Delta OPEX_F$. This has to be assessed case by case because both $\Delta OPEX_E$ and $\Delta OPEX_F$ depend on a number of factors including the specific network topology and the energy saving strategy in use. In the next section we carry out a case study on EDFAs for a specific network scenario and elaborate the maximum allowable reliability performance decrease by putting the amplifiers in sleep mode.

4.4.2 Case study

This section presents a case study where the maximum allowable failure rate increase and the potential energy saving obtained using the Weighted Power

Aware – Lightpath Routing (WPA-LR) algorithm [39] is assessed in a European backbone network, i.e., COST 239 [37].

In general, power aware RWA schemes try to minimize the network energy consumption by maximizing the number of unused fiber links so that their respective EDFAs can be put in sleep mode. The WPA-LR algorithm uses the same intuition. More specifically WPA-LR bases its RWA decisions on whether or not a given fiber link is already used to carry the traffic. If a fiber link is not in use, its routing cost is set to the power necessary to operate all the EDFAs deployed along its length (i.e., its energy consumption). If, on the other hand, a fiber link is in use its routing cost becomes the product of the fiber link power and a parameter α that varies in a range [0;1]. Values of α close to 0, encourage WPA-LR to select routes at minimum energy cost, while with 0<α<1 WPA-LR tends to make routing choices that are a compromise between energy consumption minimization and (fiber) resource efficiency maximization. More details on the WPA-LR strategy are available in [39]. This specific case study is based on the link state information (average number of active/sleeping links for a given value of the network load) gathered as a result of the WPA-LR strategy, and it uses them to calculate the achievable energy savings (focusing only on EDFAs contribution). These energy savings results are then used and to assess the maximum allowable failure rate increase for the EDFAs in the network.

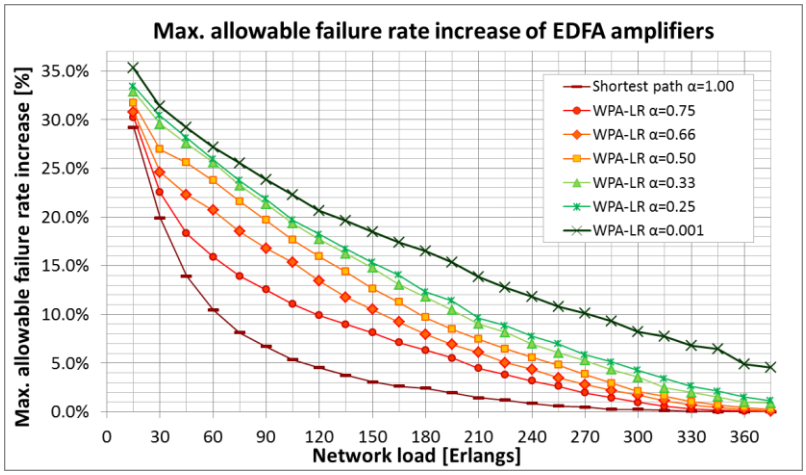

Figure 4-4: Maximum allowable failure rate increase of EDFA.

Figure 4-4 presents these values as a function of α and the network load. As explained before, with α=1 WPA-LR behaves as Shortest Path routing algorithm with First Fit wavelength assignment. The maximum allowable failure rate increase is relatively low and it decreases rapidly with the increasing load values (i.e., when there are lower chances to save energy by putting EDFAs to sleep). On the other hand, with values of α close to 0 higher values of the maximum allowable failure rate increase can be observed. Regardless of the value of α, the observed maximum allowable failure rate increase is well within the range typical for SoC, confirming our expectation mentioned in the previous section.

5 Summary

This deliverable considered the power consumption in the core transport network. In section 2, we examined power consumption optimization in flex-grid networks. Strategies investigated for power consumption optimization included hibernating operation, non-uniform traffic allocation, and dynamic traffic and spectral allocation. We developed a spectral allocation program for this deliverable, based on our existing routing and wavelength allocation program. We have developed an initial working version of flex-grid, and started on the fixed-grid model. These will be further developed as the project progresses and the results shall be reported in later deliverables.

In section 3, we developed a power consumption model for the flex-grid DISCUS network. These include the flex-grid ROADMs and MPLS-TP switches in the photonic and packet transport layers respectively, starting from network functionalities and components at system board level. These allow the network power consumption to be calculated once the nodes and links configuration is known. A detailed functional block diagram was created for flex-grid ROADM, configurable transponders and MPLS-TP switches considering all equipment functions required to support the network services envisaged in deliverable D6.1. The components or functions were grouped into boards according to the system technology state of the art and the predictable future improvements. Finally, the power model of each board was developed based on power consumption data available in the literature or extrapolated from systems data sheets.

In section 4 we described energy efficient resilient strategies for core networks that leverage on the inherent tradeoff between level of achievable power savings and other important network performance parameters such as cost, blocking probability, and the actual level of protection. We also considered impact of energy efficient strategies, such as frequent component state transition, on lifetime of core components.

In conclusion, it should be noted that this deliverable is only a preliminary deliverable and the above work are at present three separate analyses by three different partners that have made different assumptions about equipment and network parameters. These will be converged on to a common DISCUS core network design in future deliverables.

6 References

[1] M. P. Mills, “The cloud begins with coal, big data, big networks, big infrastructure, and big power”, August 2013. http://www.tech-pundit.com/

[2] Greenpeace, ”How Clean is Your Cloud?”, 2012.

[3] Gangxiang Shen and Rodney S. Tucker, “Energy-Minimized Design for IP Over WDM Networks”, J. Opt. Commun. Networks, Vol. 1, No. 1, pp. 176-186 June 2009.

[4] J. Baligan, K. Hinton, and R. S. Tucker, “Energy consumption of the Internet,” in Proc. COIN/ACOFT, Melbourne, Australia, 2007.

[5] Global Action Plan Report, An inefficient truth, 2007.

[6] K. Kawamoto, J. Koomey, B. Nordman, R. Brown, M. Piette, M. Ting, and A. Meier, “Electricity used by office equipment and network equipment in the US: detailed report and appendices,” Technical Report LBNL-45917, Energy Analysis Department, Lawrence Berkeley National Laboratory, Feb. 2001.

[7] Gartner's study of April 2007 http://www.gartner.com/it/page.jsp?id=503867.

[8] SMART 2020 Report, Enabling the low carbon economy in the information age, http://www.theclimategroup.org, 2008.

[9] O. Gerstel, M. Jinno, A. Lord, S. J. B. Yoo, "Elastic Optical Networking: A New Dawn for the Optical Layer?" IEEE Communications Magazine, issue 2, pp. s12-s20, 2012.

[10] M. Jinno, H. Takara, B. Kozicki, Y. Tsukishima, Y. Sone and S. Matsuoka, “Spectrum-Efficient and Scalable Elastic Optical Path Network: Architecture, Benefits, and Enabling Technologies”, IEEE Communications Magazine, Vol. 47, pp. 66-73.

[11] “Scalable, Tunable and Resilient Optical Networks Guaranteeing Extremely-high Speed Transport (STRONGEST)” project: http://www.ict-strongest.eu/.

[12] F. Farjady et. al., “Cost-effective upgrade of WDM all-optical networks using overlay fibres and hop reduction links,” European Transactions on telecommunications, vol. 21, no. 1, pp. 563, 2010.

[13] S. Syed, R. Rao, M. Sosa, B. Lu, B. Basch, A. G. Malis, "A Framework for control of Flex Grid Networks", IETF RFC Draft, Oct. 2012

[14] Y. Li, F. Zhang, and R. Casellas, “Flexible grid label format in wavelength switched optical network,” IETF RFC Draft, July 2011.

[15] ITU-T G.694.1, "Spectral grids for WDM applications: DWDM frequency grid," May 2002.

[16] M. Klinkowski, M. Ruiz, L. Velasco, D. Careglio, V. Lopez, and J. Comellas, "Elastic Spectrum Allocation for Time-Varying Traffic in FlexGrid Optical Networks", IEEE Selected Areas in Communications, pp. 1-12, 2011.

[17] Y. Kim et. al., "IP-Over-WDM Cross-Layer Design for Green Optical Networking With Energy Proportionality Consideration," Journal of Lightwave Technology, vol. 30, pp. 2088-2096, 2012.

[18] Deliverable D7.2. from (DISCUS Project) "The DIStributed Core for unlimited bandwidth supply for all Users and Services" http://www.discus-fp7.eu/

[19] "Reducing the Net Energy Consumption in Communications Networks by up to 90% by 2020", A GreenTouch White Paper, June 26, 2013.

[20] STRONGEST deliverable D2.4 " Final results on novel packet based Petabit transport networks fulfilling scalability, quality, cost and energy efficiency requirements "

[21] Fujitsu white paper "Path to 400G", www.fujitsu.com/downloads/TEL/fnc/whitepapers/Pathto400G.pdf

[22] Finisar product brief "Finisar DWPf 1x9 and 1x20 WSS Dynamic Wavelength Processor (DWP)" http://www.finisar.com/

[23] Ciena Optical Amplifiers specifications http://www.ciena.com/products/optical-amplifier/tab/specs

[24] Civcom product brief "100G DP-QPSK Coherent Tunable Transponder" http://civcom.com/

[25] A. Morea, S. Spadaro, O. Rival, J. Perelló, F. Agraz, D. Verchere, Power Management of Optoelectronic Interfaces for Dynamic Optical Networks, paper We.8.K.3 ECOC 2011.

[26] A. Muhammad et al., "Energy-efficient WDM network planning with dedicated protection resources in sleep mode," in Proc. IEEE GLOBECOM, 2010.

[27] F. Musumeci et al., "Energy-efficiency of protected IP-over-WDM networks with sleep-mode devices," J. High Speed Networks, vol. 19, no. 1, pp. 19–32, 2013.

[28] A. Morea et al., "Power management of optoelectronic interfaces for dynamic optical networks," in ECOC proc. IEEE, 2011, pp. 1–3.

[29] P. Monti et al., "Energy-efficient lightpath provisioning in a static WDM network with dedicated path protection," in Proc. ICTON, 2011.

[30] A. Jirattigalachote et al., "Dynamic provisioning strategies for energy efficient WDM networks with dedicated path protection," Optical Switching and

Networking, vol. 8, no. 3, pp. 201–213, 2011.

[31] C. Cavdar et al., "Energy-efficient design of survivable WDM networks with shared backup," in GLOBECOM, 2010.

[32] S. S. Jalalinia, "Survivable green optical backbone networks with shared path protection," Master Thesis, KTH Royal Institute of Technology, Dec. 2012.

[33] N.-H. Bao et al., "Power-aware provisioning strategy with shared path protection in optical WDM networks," Optical Fiber Technology, vol. 18, no. 2, pp. 81–87, 2012.

[34] J. Y. Yen. Management Science, vol. 17, no. 11, pp. 712-716, July 1971.

[35] R. He et al., "Dynamic power-aware shared path protection algorithms in WDM mesh networks," J. of Comm., vol. 8, no. 1, pp. 55–65, 2013.

[36] C. Ou, J. Zhang, L. H. Sahasrabuddhe, and B. Mukherjee, J. Lightw. Technol., vol. 22, no. 5, pp.1223-1232, May 2004.

[37] P. Batchelor et al., Photonic Network Commun., vol. 2, pp. 15–32, 2000.

[38] S. Aleksić, J. Opt. Commun. Netw., vol. 1, no. 3,pp. 245–258, 2009.

[39] P. Wiatr and et al., "Power savings versus network performance in dynamically provisioned wdm networks," *IEEE Communication Magazine*, vol. 50, no. 54, pp. 48–55, May 2012.

[40] A. Fumagalli and et al., "Differentiated reliability (DiR) in WDM rings without wavelength converters," in ICC proc., 2001.

[41] P. Monti and et al., "Resource-efficient path-protection schemes and online selection of routes in reliable WDM networks," J. Opt. Netw., vol. 3, no. 4, pp. 188–203, Apr 2004.

[42] J.L. Vizcaino and et al.,"Differentiated quality of protection to improve energy efficiency of survivable optical transport networks," in OFC proc., 2013.

[43] A. Muhammad, and et al. "Reliability Differentiation in Energy Efficient Optical Networks with Shared Path Protection," in Proc. of IEEE Online Conference on Green Communication, October 29-31, 2013.

[44] V. Jimenez and et al., "Computing the k shortest paths: A new algorithm and an experimental comparison," Springer, vol. 1668, pp. 15–29, 1999.

[45] Z. Yi et al., *"Energy Efficiency in Telecom Optical Networks,"* IEEE Communications Surveys & Tutorials, Q4 2010.

[46] P. Wiatr et al., *"Energy saving in access networks: Gain or loss from the cost perspective?,"* ICTON 2013, June 2013.

[47] W. Engelmeier, "*Solder Joints in Electronics: Design for Reliability*".

[48] K. Setty et al., *"Powercycling Reliability, Failure Analysis and Acceleration Factors of Pb-Free Solder Joints,"* 55th Conference on Electronic Components and Technology, May/June 2005.

[49] A. Coiro et al., "Power-Aware Routing and Wavelength Assignment in Multi-Fiber Optical Networks," IEEE/OSA JOCN, Nov. 2011.

[50] P. Wiatr et al., "Energy Efficiency and Reliability Tradeoff in Optical Core Networks," in Proc. of IEEE/OSA Optical Fiber Communication Conference and Exposition (OFC), March 9-13, San Francisco, USA, 2014.

[51] A. Leiva et al., "Upgrading cost modeling of capacity-exhausted static WDM networks," ONDM 2012, April 2012.

[52] Optical Access Seamless Evolution (OASE), FP7 project, http://www.ict-oase.eu/.

[53] The DIStributed Core for unlimited bandwidth supply for all Users and Services (DISCUSs), FP7 project, http://www.discus-fp7.eu/.

[54] T.S. Rosing et al., "Power and Reliability Management of SoCs," IEEE Transactions on VLSI Systems, Apr. 2007.

7 Abbreviations

A/D	Add/Drop
APS	Automatic Protection Switching
ASC	Amplified Splitter and Couplers
C-band	Band in the wavelength range 1530–1565 nm
CO2	Carbon Dioxide
COST 239	Ultra-High Capacity Optical Transmission Networks
DiR	Differentiated Reliability
DISCUS	The DIStributed Core for unlimited bandwidth supply for all Users and Services
DP	Dual Polarization
DP-BPSK	Dual Polarization Binary Phase-Shift Keying
DP-QPSK	Dual Polarization Quaternary Phase-Shift Keying
DWDM	Dense Wavelength Division multiplexer
EASPP	Energy-aware shared path protection
EDFA	Erbium Doped Fibre Amplifier
EOP	Elastic Optical Path
EUSPP	energy-unaware shared path protection
EUSPP-NS	EUSPP where backup resources being active
EUSPP-S	EUSPP where backup resources are in sleep mode
FIT	Failure in Time
GE	Gigabit Ethernet
GHG	Green House Gases
ICT	Information Communications Technology
IETF	Internet Engineering Task Force
ITU	International Telecommunications Union
ITU-T	ITU's Telecommunication Standardization Sector
MCFP	Maximum conditional failure probability
MPLS-TP	Multi-Protocol Label Switching Transport Profile
MSA	Multi-Source Agreement
MSC	Multicast Switch
MtCO2e	Million metric tons of carbon dioxide equivalent.

	This measure can aggregate different greenhouse gases into a single measure, using global warming potentials. One unit of carbon is equivalent to 3.664 units of carbon dioxide.
MTTR	Mean Time To Repair
NP-Complete	Nondeterministic polynomial
OEO	Optical-Electronic-Optical (conversion)
OPEX	Operational Expenditure
OPM	Optical Performance Monitoring
OSC	Optical Supervisory Channel
OSNR	Optical signal to Noise Ratio
P_BCB	Power Consumption of Basic control of board
P_MSC	Power Consumption of MSC module (any type)
P_OAB	Power Consumption of EDFA dual stage variable gain (booster)
P_OAN	Power Consumption of EDFA small gain amplifier for ASC and MSC (single fibre)
P_OAP	Power Consumption of EDFA single stage fixed gain (preamplifier)
P_OSC	Power Consumption of Optical Supervisory Channel
P_OPM	Power Consumption of Optical Performance Motoring
P_WSS	Power Consumption of WSS module (any type)
PC	Personal Computers
QAM	Quadrature Amplitude Modulation
QoS	Quality of Service
QPSK	
ROADM	Re-configurable Optical Add Drop Multiplexer
RWA	Routing and Wavelength Allocation
SoC	System on Chip
SPF	shortest path first
SPP	shared path protection
STRONGEST	Fp7 project “Scalable, Tunable and Resilient Optical Networks Guaranteeing Extremely-high Speed Transport”
TWh	Terawatt-Hour
WDM	Wavelength Division Multiplexing
WP	Work Package

WPA-LR	Weighted Power Aware – Lightpath Routing
WSS	Wavelength Selective Switch